UMTA-MA-06-0025-83-2
DOT-TSC-UMTA-83-1

Wheel/Rail Force Measurement at the Washington Metropolitan Area Transit Authority-Phase II

Volume II
Test Report

P.J. Boyd
J.P. Zaiko
W.L. Jordan

ENSCO, Inc.
Springfield VA 22151

June 1983
Final Report

U.S. Department of Transportation
Urban Mass Transportation Administration

Office of Technical Assistance
Office of Systems Engineering
Washington DC 20590

Technical Report Documentation Page

1. Report No.	2. Government Accession No.	3. Recipient's Catalog No.
UMTA-MA-06-0025-83-2		

4. Title and Subtitle	5. Report Date
WHEEL/RAIL FORCE MEASUREMENT AT THE WASHINGTON METROPOLITAN AREA TRANSIT AUTHORITY - PHASE II VOLUME II TEST REPORT	June 1983
	6. Performing Organization Code: TSC/DTS-77
7. Author(s): P.J. Boyd, J.P. Zaiko, and W.L. Jordan	8. Performing Organization Report No.: DOT-TSC-UMTA-83-1
9. Performing Organization Name and Address: ENSCO, INC.* Transportation Technology Engineering Division 5400 Port Royal Road Springfield, VA 22151	10. Work Unit No. (TRAIS): UM204/R2608
	11. Contract or Grant No.: DTFR-53-80-C-00002
12. Sponsoring Agency Name and Address: U.S. Department of Transportation Urban Mass Transportation Administration Office of Technical Assistance Washington, DC 20590	13. Type of Report and Period Covered: Final Report May 1981-November 1981
	14. Sponsoring Agency Code: URT-10

15. Supplementary Notes

*Under contract to: U.S. Department of Transportation
Research and Special Programs Administration
Transportation Systems Center
Cambridge, MA 02142

16. Abstract

On the basis of preliminary studies, modification of the subway cars of the Washington Metropolitan Area Transit Authority for softer longitudinal primary suspension and tapered wheels was suggested to reduce excessive wheel and rail wear and rail fastener failure.

Force sensing instrumented wheels and other sensors were used to measure the effects of wheel taper and longitudinal stiffness of the primary suspension. Both changes reduced curving flange forces. Suspension compliance had the predominant effect at curves of less than 1000 ft radius, and wheel taper produced the greatest reduction of flange force at larger curves. The combination of both changes was complimentary. Reductions in lateral force of 60%-90% relative to the standard truck were achieved with 1:20 tapered wheels and softer suspension bushings.

No hunting was detected at 75 mph with up to 1:10 wheel taper for either the standard or soft primary longitudinal suspension.

Volume I of this Test Phase report carries the sub-title of Analysis Report.

17. Key Words	18. Distribution Statement
Wheel/Rail Forces Wheel/Rail Wear Urban Transit Vehicle Instrumented Wheels	DOCUMENT IS AVAILABLE TO THE PUBLIC THROUGH THE NATIONAL TECHNICAL INFORMATION SERVICE, SPRINGFIELD, VIRGINIA 22161

19. Security Classif. (of this report)	20. Security Classif. (of this page)	21. No. of Pages	22. Price
UNCLASSIFIED	UNCLASSIFIED	94	

Form DOT F 1700.7 (8-72) Reproduction of completed page authorized

PREFACE

In support of the Office of Rail and Construction Technology of the Urban Mass Transportation Administration (UMTA), the Transportation Systems Center (TSC) is conducting analytical and experimental studies to relate transit truck design characteristics, wheel/rail forces and wheel/ rail wear rates, in order to provide options for reducing the wear rates of wheels and rails experienced by transit properties and minimizing system life cycle costs of vehicle and track components, while maintaining or improving equipment performance.

As part of this work, TSC planned and implemented a measurement program, in order to obtain onboard wheel/rail force measurements over a representative range of Washington Metropolitan Area Transit Authority (WMATA) operating conditions; obtain data to quantify the load environment on direct fixation fasteners and evaluate the influence of changes in fastener characteristics on fastener performance; evaluate the influence of taper and suspension modifications on high speed stability and to assess the feasibility of a retrofit to the WMATA truck to improve curving performance. These tests were conducted in the fall of 1981. The Analytic Sciences Corporation (TASC), under Contract DTRS-57-80-C-00062, provided support to TSC in these activities, by conducting analyses of the tradeoffs between curving performance and high speed stability, by definition and coordination of in-shop measurements to obtain engineering parameters for use in the analysis, by specification and procurement of the retrofit primary suspension element used in the truck tests, by comparison of measured data, with analytic predictions to assess measurement consistency and by recommending test program modifications to improve the accuracy and completeness of the results relating to the truck modifications. This report describes the work performed by TASC under this effort in support of this measurement program. The report Number is UMTA-MA-06-0025-83-.

Vehicle/truck instrumentation and data acquisition support for the truck tests was provided by ENSCO, Inc., while equipment and support personnel, for conducting selected vehicle and truck measurements in the WMATA shop, were provided by the Transportation Test Center (TTC), Pueblo, Colorado and are provided in this report. The modified primary suspension elements used in the (Phase II) test program were developed and fabricated by the BUDD Co., under subcontract to and in accordance with design specifications developed by TASC. Vehicles, operators, track rights, shop facilities and shop test support were provided by WMATA.

Wayside instrumentation development, installation and calibration and data acquisition support for measurements of fastener loads was provided by Battelle Columbus Labs, under contractual arrangement with TSC. Results of these measurements will be documented in subsequent reports.

METRIC CONVERSION FACTORS

Approximate Conversions to Metric Measures

Symbol	When You Know	Multiply by	To Find	Symbol
		LENGTH		
in	inches	*2.5	centimeters	cm
ft	feet	30	centimeters	cm
yd	yards	0.9	meters	m
mi	miles	1.6	kilometers	km
		AREA		
in^2	square inches	6.5	square centimeters	cm^2
ft^2	square feet	0.09	square meters	m^2
yd^2	square yards	0.8	square meters	m^2
mi^2	square miles	2.6	square kilometers	km^2
	acres	0.4	hectares	ha
		MASS (weight)		
oz	ounces	28	grams	g
lb	pounds	0.45	kilograms	kg
	short tons (2000 lb)	0.9	tonnes	t
		VOLUME		
tsp	teaspoons	5	milliliters	ml
Tbsp	tablespoons	15	milliliters	ml
fl oz	fluid ounces	30	milliliters	ml
c	cups	0.24	liters	l
pt	pints	0.47	liters	l
qt	quarts	0.95	liters	l
gal	gallons	3.8	liters	l
ft^3	cubic feet	0.03	cubic meters	m^3
yd^3	cubic yards	0.76	cubic meters	m^3
		TEMPERATURE (exact)		
°F	Fahrenheit temperature	5/9 (after subtracting 32)	Celsius temperature	°C

*1 in = 2.54 (exactly). For other exact conversions and more detailed tables, see NBS Misc. Publ. 286, Units of Weights and Measures, Price $2.25, SD Catalog No. C13.10:286.

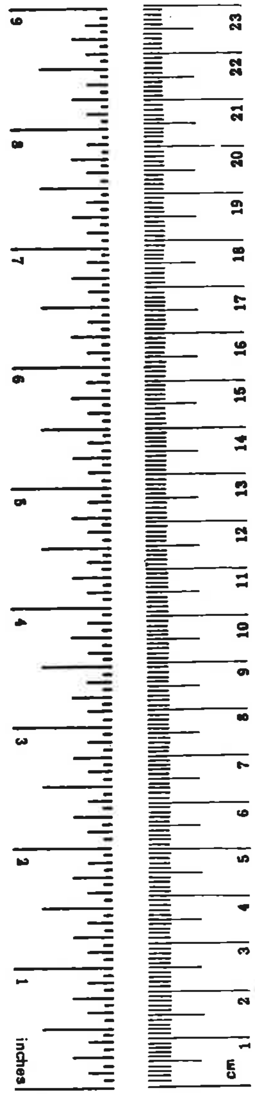

Approximate Conversions from Metric Measures

Symbol	When You Know	Multiply by	To Find	Symbol
		LENGTH		
mm	millimeters	0.04	inches	in
cm	centimeters	0.4	inches	in
m	meters	3.3	feet	ft
m	meters	1.1	yards	yd
km	kilometers	0.6	miles	mi
		AREA		
cm^2	square centimeters	0.16	square inches	in^2
m^2	square meters	1.2	square yards	yd^2
km^2	square kilometers	0.4	square miles	mi^2
ha	hectares (10,000 m^2)	2.5	acres	
		MASS (weight)		
g	grams	0.035	ounces	oz
kg	kilograms	2.2	pounds	lb
t	tonnes (1000 kg)	1.1	short tons	
		VOLUME		
ml	milliliters	0.03	fluid ounces	fl oz
l	liters	2.1	pints	pt
l	liters	1.06	quarts	qt
l	liters	0.26	gallons	gal
m^3	cubic meters	35	cubic feet	ft^3
m^3	cubic meters	1.3	cubic yards	yd^3
		TEMPERATURE (exact)		
°C	Celsius temperature	9/5 (then add 32)	Fahrenheit temperature	°F

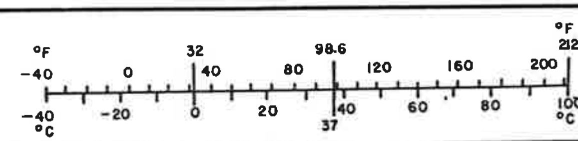

TABLE OF CONTENTS

LIST OF ILLUSTRATIONS

LIST OF TABLES

1.0 INTRODUCTION

The Washington Metropolitan Area Transit Authority (WMATA) has experienced high rates of wear of wheels and rails and failures of rail fasteners. These problems are especially pronounced on curves having radii less than one thousand feet (5.7^{o}). Preliminary studies conducted by the Transportation Systems Center (TSC) (ref) and by Deleuw, Cather and Company (ref) recommended several changes to the vehicles and track. This report describes a test program to evaluate the effect of the recommended changes to the WMATA car on curving flange forces and high speed stability. The participating agencies were the Urban Mass Transit Administration (UMTA), TSC, ENSCO, the Analytic Sciences Corporation, Battelle Columbus Laboratories, WMATA, and the Federal Railroad Administration (FRA).

The test directly addresses the classical trade off between curving and stability. The use of highly tapered wheels and longitudinally compliant primary suspension allows a vehicle to negotiate sharper curves without flange contact or excessive slip. Increasing the taper reduces the axle movement toward the high rail necessary to maintain pure rolling in a curve, and longitudinal compliance allows the axles to orient radially to the curve. However, both taper and compliance reduce the speed at which unstable "hunting" occurs. Wheel taper causes the varying lateral component of the contact force which drives the oscillation, and compliance partially uncouples the wheelsets from the truck frame creating a less stable system.

The possibility that the original truck design compromised curving to gain excessive stability, in view of the actual speed and curving requirements, motivated this test in which wheel taper and primary suspension stiffness were the principal variables. Tapers of zero (cylindrical wheel), 1:20, 1:10 and 1:5 were used. Testing with 1:5 taper was cancelled, however, because yard movements demonstrated the inability of the switch frogs to handle steeply tapered wheels. The primary suspension of the Rockwell Trucks used at WMATA consisted of an elastomeric bushing with a longitudinal stiffness of 115,000 lb/in (vertical, 74,000 lb/in; lateral, 62,000 lb/in). An experimental bushing constructed for greater longitudinal compliance with a longitudinal stiffness of 29,700 lb/in (vertical, 116,00 lb/in; lateral, 37,000 lb/in) was also used to vary the radial self-steering property of the truck. The test was divided into series featuring different combinations of the two mechanical variables as shown in Table 1-1.

TABLE 1-1

TEST SERIES

Series	Wheel Taper	Primary Suspension Longitudinal Stiffness
A	cyl.	115,00 lb/in
B	1:20	115,000 lb/in
C	1:10	115,000 lb/in
D*	1:5	115,000 lb/in
F	1:10	29,700 lb/in
G	1:20	29,700 lb/in
I**	1:20	115,000 lb/in
J	cyl.	29,700 lb/in

* Cancelled due to insufficient switch frog clearance.

**100 passes over curve 37 in Series B configuration to investigate the possibility of rail contamination.

2.0 DESCRIPTION OF TESTS

The Brentwood Shop facility served as the base of operations for all testing. Most of the tests were conducted on the Red Line (Van Ness-Silver Spring) which is adjacent to the Brentwood yard.

2.1 STEADY CURVING

The steady curving tests were performed by driving a married pair of vehicles from Farragut North to Brookland on the Red Line as indicated in Figure 2-1. The speed was held as constant as possible at six test curves along the route. Several passes over the entire route were made to provide a range of speed levels at each test curve. The speed was limited to the service speed at each curve by the automatic train control system. The instrumented wheelset was in the lead position of the first car for forward runs and in the trailing position of the last car for the reverse runs.

Table 2-1 identifies the test curves. They range in radii from 755 ft. to 2508 ft. with a radius of less than 1000 ft. for three test curves. All curves except 311 were turning left in the forward test direction. Superelevation typically was held to 4 inches in tunnels for clearance.

The listed service speeds were not exceeded during testing, but up to 4.5 inches of cant deficiency could be developed at representative sharp right and left curves. Curve 37 was equipped with force sensing instrumented rails to monitor revenue traffic as part of a simultaneous track oriented program also conducted by TSC. Very good agreement, especially at the heavily flange loaded high rail, was obtained between the independent wayside and onboard measurements.

The route evaluation runs listed in Appendix B were steady curving tests in which the speed was controlled by the autopilot rather than manual override. The maximum test speeds usually occurred during route evaluation runs.

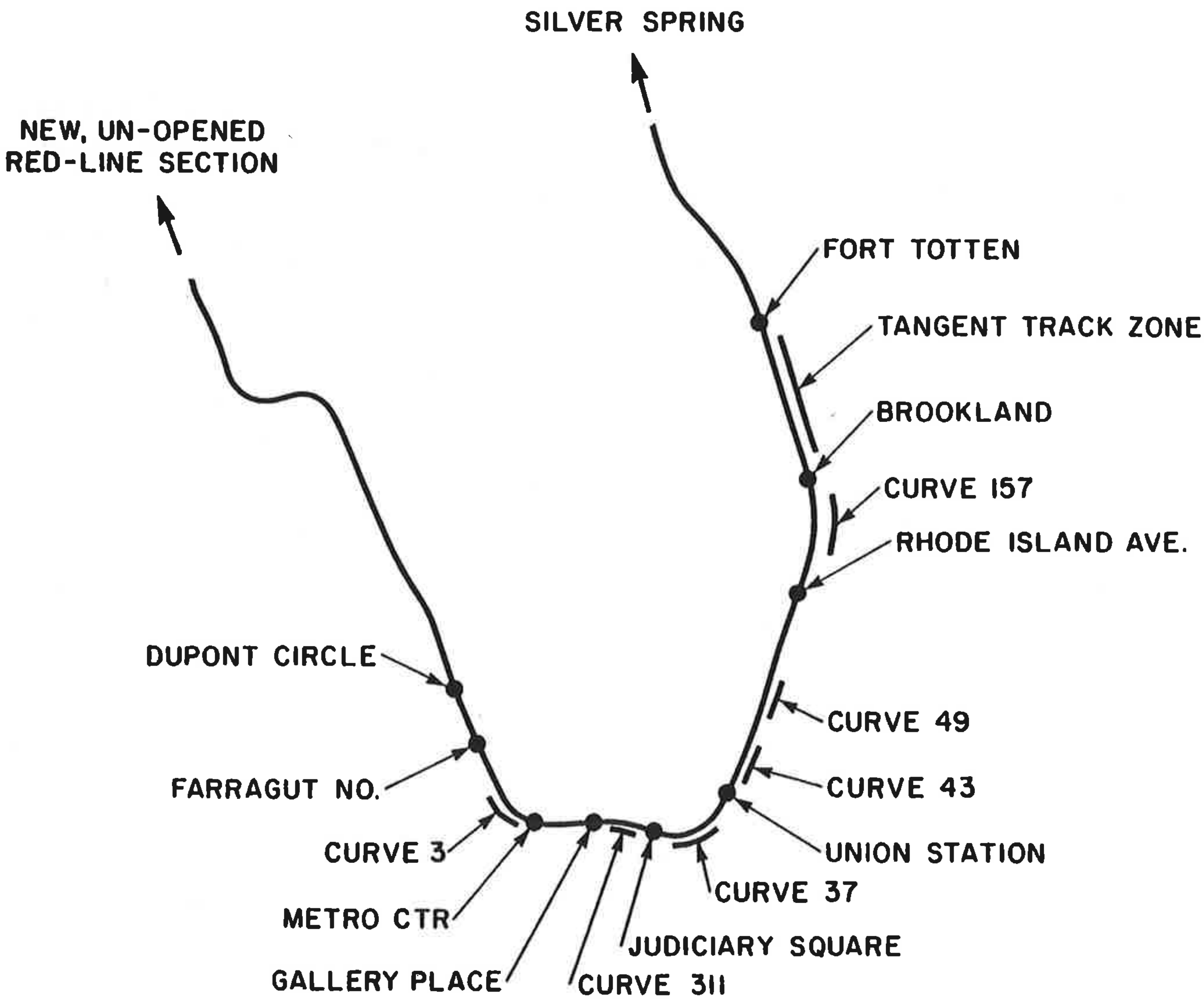

FIGURE 2-1. ROUTE DESCRIPTION

TABLE 2-1

TEST CURVES

No.	Length (ft)	Radius (ft)	Curvature (deg)	S.E. (in)	Service Speed (mph)	Cant Deficiency at Service Speed (in)
3	490	1200	4.8	4	50	4.4
311	430	956	6.0	4	45	4.5
37	780	755	7.6	4	40	4.5
43	220	1750	3.3	6	65	3.7
49	310	800	7.2	6	45	4.2
157	680	2508	2.3	6	70	1.8

A special set of steady curving tests were performed at curve 6 on the Blue Line because its rails had substantially less wear than those at the older Red Line curves.

2.2 ACCELERATION IN CURVES

A mode of non-steady curving was also tested. The vehicle was stopped on tangent track before the test curve, and a traction motor current control setting was selected. The vehicle then accelerated through the curve with constant tractive effort. The test was repeated at the highest and next to highest current control levels. Curves 3, 37, and 157 were used as test sites.

2.3 STABILITY TESTS

A tangent track zone between Fort Totten and Brookland on the Red Line (Figure 2-1) was selected for stability tests. The maximum speed of the transit system, 75 mph, is permitted in this zone.

Each combination of taper and suspension bushing stiffness was run at 35, 55, 65 and 75 mph in both directions. Wheelset to truck frame yaw and lateral displacement, truck to carbody yaw and lateral displacement, and axle lateral acceleration were observed for signs of unstable oscillation.

2.4 SYSTEM SURVEYS

In addition to the performance tests on the Red Line during out of service hours, the test cars were run over the entire system during Sunday revenue service. Both tracks of the Red, Orange and Blue Lines were traversed with the instrumented truck leading. The test train ran between scheduled trains under autopilot control.

The survey was performed twice. The standard configuration of stiff bushings and cylindrical wheels and an experimental configuration of soft bushings and 1:20 tapered wheels were used.

3.0 VEHICLE INSTRUMENTATION

The vehicle was equipped with instruments to measure, display and record the following parameters:

1. Vertical and lateral wheel/rail forces at each wheel on the lead axle.
2. Lateral acceleration of each axle on the lead truck and the lead axle of the trailing truck.
3. Longitudinal deflections of each primary suspension bushing of the lead truck.
4. Lateral deflection of each primary suspension bushing of the lead truck.
5. Vertical and lateral acceleration of a traction motor on the lead truck.
6. Yaw and lateral displacement of the lead truck with respect to the carbody.
7. Carbody lateral acceleration, vertical acceleration, and roll acceleration
8. Vehicle speed
9. Traction motor current of one truck
10. Simultaneously recorded track location reference marks

3.1 TRANSDUCERS

Most of the transducers were mounted on the lead truck of the lead car. They are briefly described below in the same order in which the parameters they measure were listed. The force sensing wheelset was the most elaborate transducer and it is described in detail in the next section. Figure 3-1 locates the truck mounted transducers by the numbers of the headings of the following descriptions.

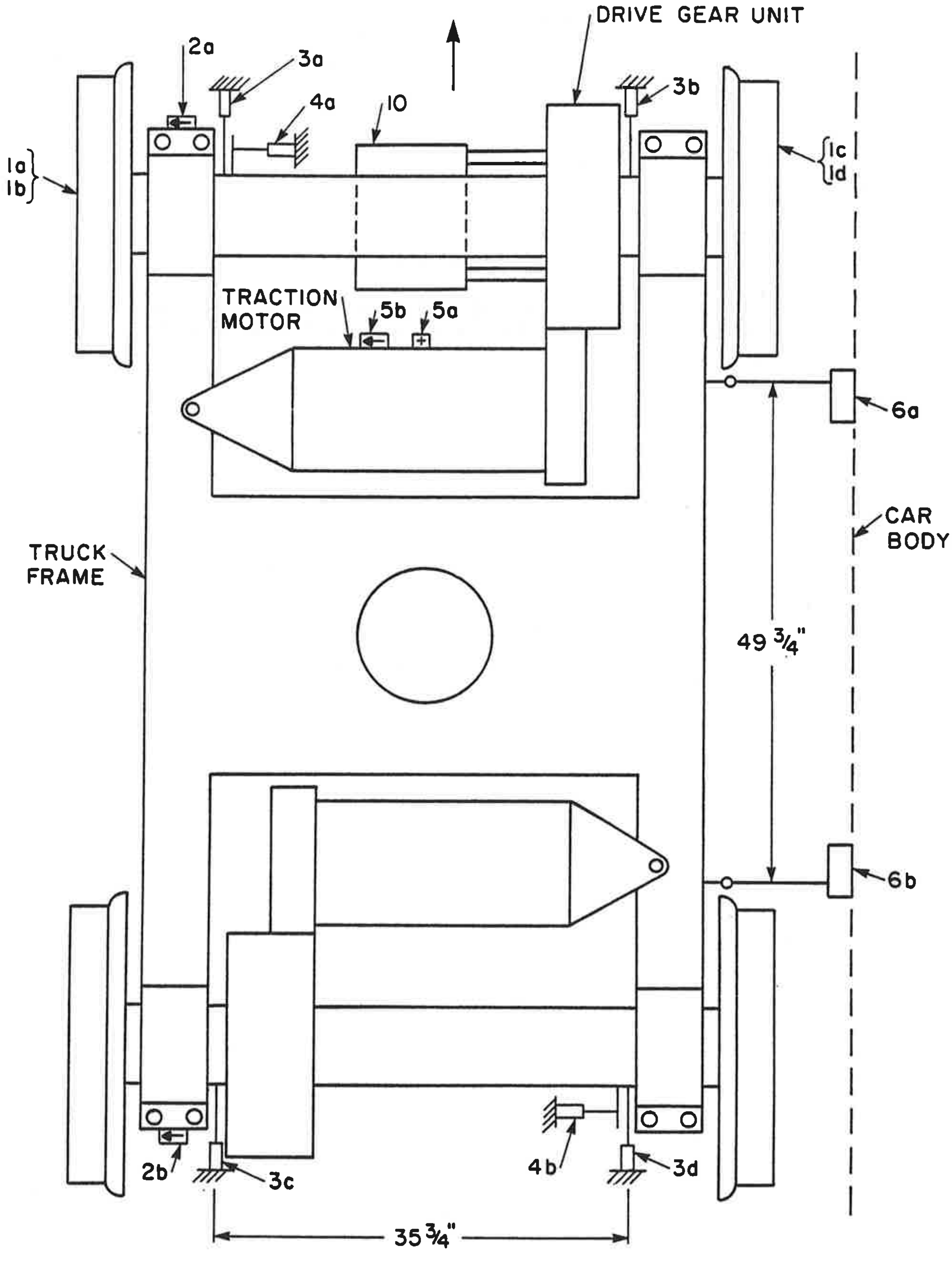

FIGURE 3-1. SENSOR PLACEMENT ON LEAD TRUCK

1. a) Left front wheel vertical force - a pair of strain gage bridges on the wheelplate producing triangular wave strain summations as the wheel rotates. A wheelset processor combines the output of the two out of phase bridges to create a single continuous signal proportional to vertical force. See Section 3.2 for details.

   b) Left front wheel lateral force - a similar pair of strain gage bridges on the wheelplate producing sinusoidal strain summations as the wheel rotates under a lateral load. A wheelset processor combines the output of the two out of phase bridges to create a single continuous signal proprotional to lateral forces. See Section 3.2 for details.

   c) Right front wheel vertical force - same as left sensor

   d) Right front wheel lateral force - same as left sensor

2. a) Lead truck - lead axle lateral acceleration - 5g servo accelerometer mounted to the truck frame at the axle bearing clamp.

   b) Lead truck - trailing axle lateral acceleration - similar sensor

   c) Trailing truck - lead axle lateral acceleration - similar sensor

3. a), b), c), d) primary suspension longitudinal deflection at all four axle bearings on the lead truck - DC-DC LVDT displacement transducers (min $\pm$1/2" range) acting between the bearing clamp of the truck frame and the outer race of the axle bearing.

4. a), b) Primary suspension lateral deflection for each axle of the lead truck - DC-DC LVDT displacement transducers (min $\pm$1/2" range) acting between the bearing clamp of the truck frame and the outer race of one bearing on each axle.

5. a. Vertical acceleration of lead traction motor - 5g servo accelerometer mounted to the front face of the traction motor.

   b) Lateral acceleration of the lead traction motor - similar sensor.

6. a), b) String type ($\pm$5-1/2" range) displacement transducers between the right side of the body and the side of the truck frame. Truck yaw is the difference in output of the two transducers divided by their spacing; lateral translation is the average output of the sensors.

7. a) Carbody vertical acceleration - 1g servo accelerometer mounted on the car interior floor along the center line near the front truck.

   b) Carbody lateral acceleration - similar transducer and mounting

   c) Carbody roll acceleration - a second 1g vertical servo accelerometer offset laterally from 7a) provides the means in conjunction with 7a) for calculating roll acceleration.

8. Vehicle speed - a test point in the vehicle speed control circuit was used for an analog speed indication.

9. Traction motor current - a test point in the vehicle was used for an analog indication of the traction motor current for one truck.

10. Automatic Location Detection - a capacitive sensor mounted on the gear drive, cantilevered to the car centerline below the axle, produced spikes to indicate the presence of aluminum sheet metal targets placed at rail sensors or other track features. Permanent track features such as switch turnouts or electrical enclosures between the rails produced spikes to identify locations during survey runs.

3.2 INSTRUMENTED WHEELSET

The lead axle in the forward direction was equipped with wheels instrumented to sense vertical and lateral contact forces continuously. Figure 3-2 is a block diagram of the wheel/rail force measuring system. The essential elements are 1) pairs of strain gage bridges producing ac signals as the wheel rolls, proportional to lateral or vertical force, 2) slip rings to allow rotation of the electircal circuits, 3) high gain carrier amplifiers

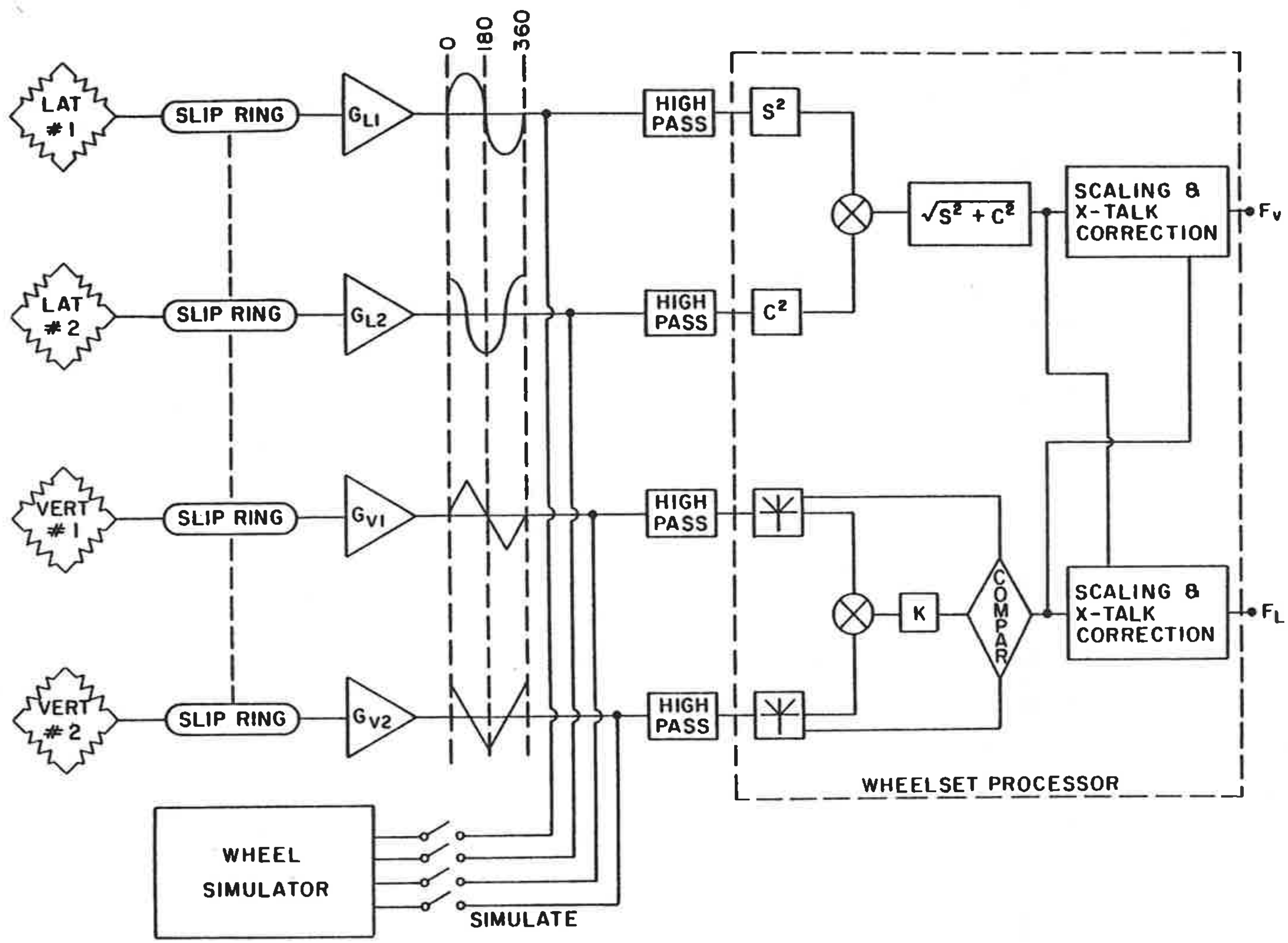

FIGURE 3-2. WHEELSET DATA FLOW

suited to bridge signals in the microvolt range, 4) high pass filters to achieve automatic zeroing, and 5) a processor to combine bridge signals into direct force indications and to perform crosstalk corrections. ENSCO has produced many wheelsets for FRA safety experiments to measure limiting values of flange force which required accuracy at high lateral forces. The WMATA car tests also required accuracy to very low lateral forces to evaluate the desired effects of wheel taper and suspension changes. Higher sensitivity of both lateral and vertical bridges and improved linearity of lateral bridges at very low force were achieved for the WMATA car, but the crosstalk was greater than for previous wheels. The crosstalk between vertical load and lateral force indication (and vice versa) were determined by calibration in a loading fixture after each change of taper, and thus accuracy was maintained through compensation performed by the processor. The basic sensitivity of the vertical and lateral bridges (microstrain per 1000 lb of load) did not change greatly during successive machinings of the wheel tread.

The basic objective of the design of force measuring wheels is to obtain adequate primary sensitivity for low signal/noise ratio and high resolution while controlling crosstalk, load point sensitivity, ripple, and the effects of heat, centrifugal force and longitudinal forces. The design philosophy was to choose strain gage bridge configurations which inherently minimized as many extraneous influences as possible and which were responsive to the general strain patterns expected in any rail wheel subjected to vertical and lateral forces. Such bridge configurations could be adapted to the standard production wheels of any test vehicle, eliminating problems of supply, mechanical compatibility, and possible alterations of vehicle behavior due to special wheels. The radial locations of the strain gages were optimized for each wheel size and shape while their angular locations were fixed by the chosen bridge configurations. Locomotive, passenger coach and freight car wheels, as well as small transit car wheels, have been instrumented successfully by ENSCO using the same general procedures.

3.2.1 DESCRIPTION OF STRAIN GAGE BRIDGES

The vertical force measuring bridges follow a concept used by ASEA/SJ. Each bridge consists of eight strain gages arranged in a Wheatstone bridge having two gages per leg. Each leg of the bridge has one strain gage on the field side and one strain gage on the gage side of the wheel. The four legs are evenly spaced 90° apart on the wheel as shown in Figure 3-3. The general strain distribution in a typical rail wheelplate due to a purely vertical load is characterized by maximum strains which are compressive and highly localized in the wheelplate above the point of rail contact. As the pair of gages in each leg of the bridge consecutively passes over the rail contact point, two negative and two positive peak bridge outputs occur per revolution. By correctly choosing the radial position of the gages, the bridge output as a function of rotational position of the wheel can be made to resemble a triangular waveform having two cycles per revolution. The purpose of having gages on both sides of the wheelplate in each leg is to cancel the effect of changes in the bending moments in the wheelplate due to lateral force and the change of axial tread/rail contact point.

When two triangular waveforms equal in amplitude and out of phase by one-fourth the wavelength, are rectified and added, the sum is a constant equal to the peak amplitude of the individual waveforms. In order to generate a strain signal proportional to vertical force and independent of wheel rotational position, the outputs of two identical vertical bridges out of phase by 45° of wheel arc are rectified and summed as shown in Figure 3-4. Since the bridge outputs do not have the sharp peaks of true triangular waveforms, the sum of one bridge peak and one bridge null is lower than that of two concurrent intermediate bridge outputs. In order to reduce the ripple or variation in force channel output with wheel rotation, the bridge sum is scaled down between the dips coinciding with the rounded bridge peaks. By taking as the force channel output the greatest of either individual bridge output or the scaled down sum of both bridges, the scaling down

"A + B" TRIANGULAR OUTPUT (ASEA/SJ)

- TWO BRIDGES
- GAGES ON BOTH SIDES OF WHEELPLATE
- TRIANGULAR WAVEFORMS - 2 - CYCLES PER REVOLUTION
- OUTPUT = MAX $\{|A|, |B|, K(|A| + |B|)\}$

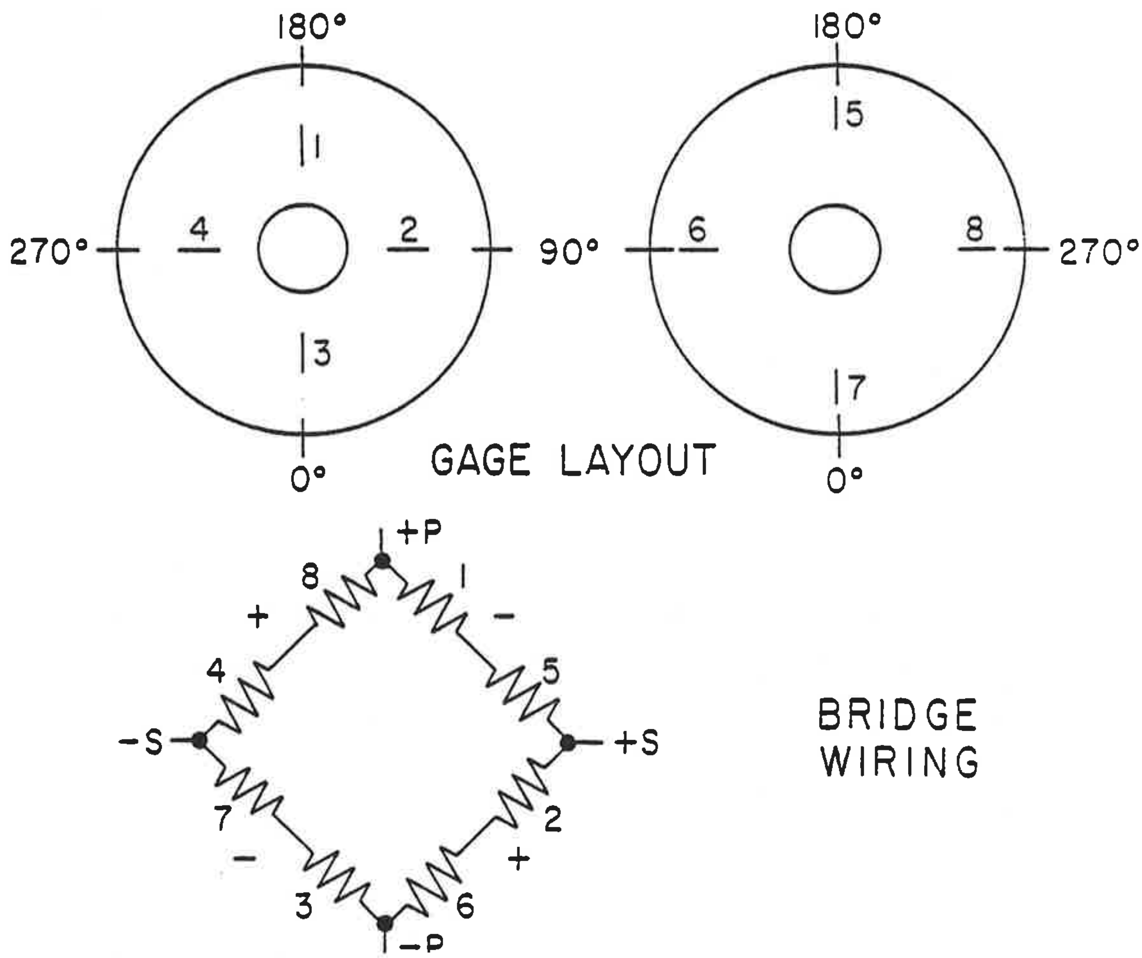

FIGURE 3-3. VERTICAL FORCE MEASUREMENT BRIDGE

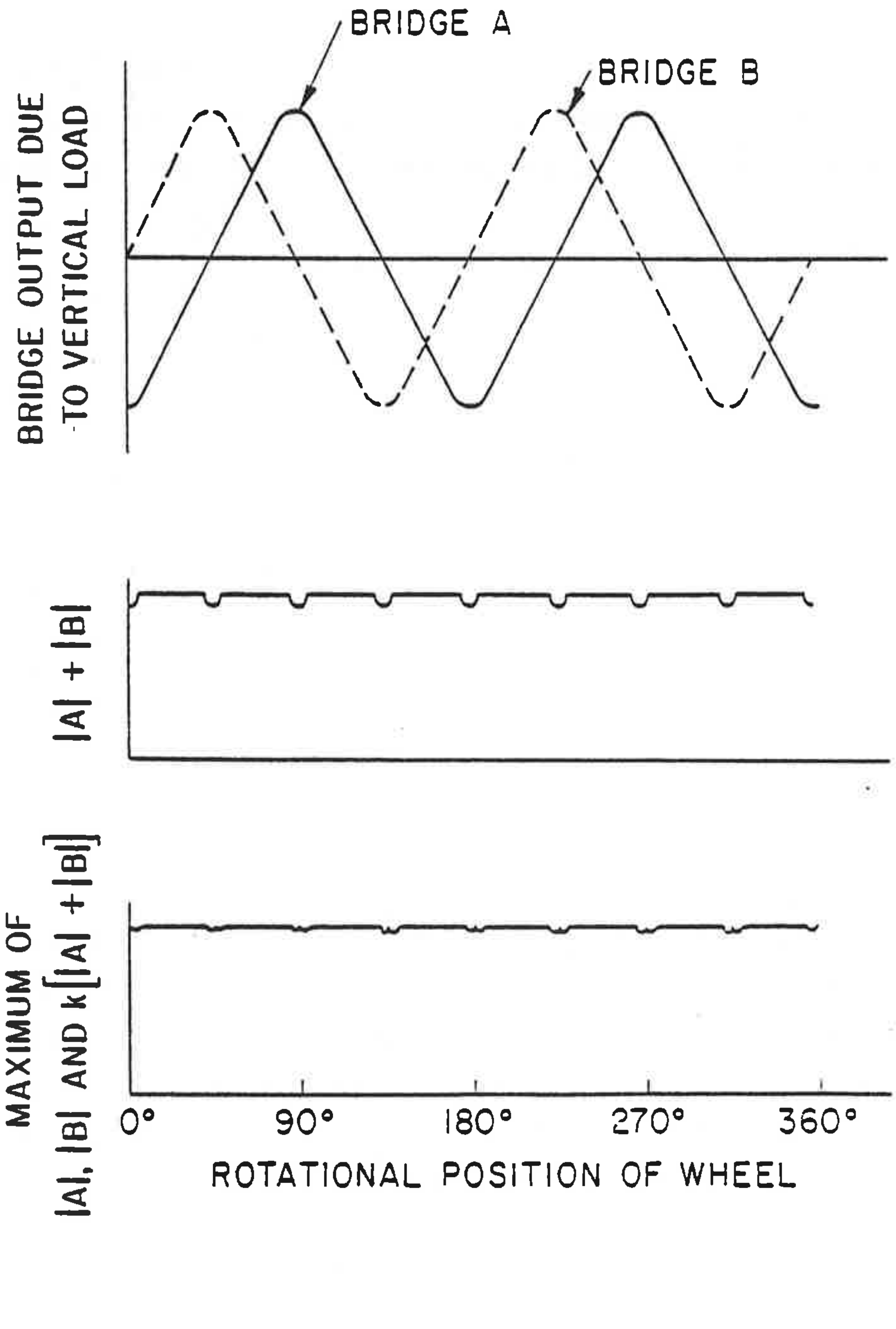

FIGURE 3-4. TRIANGULAR OUTPUT AND "A + B" PROCESSING

is applied selectively to the part of the force channel output between the dips as shown in Figure 3-4.

The general strain distribution of a typical rail wheelplate due to a purely lateral flange force is characterized by two components as shown in Figure 3-5. One component is a function of radius only because the wheelplate acts as a symmetric diaphragm in opposing the lateral force at the axle. The second component results from the moment about the hub caused by the flange force, and it tends to vary at a given radius with the cosine of the angular distance from the wheel/rail contact point. The strain distributions on the gage and field sides of the wheelplate are similar in magnitude but opposite in sign (compression or tension).

Lateral force measuring bridges which follow a concept advanced by EMD (Ref. 19) take advantage of the general strain distribution in a standard rail wheelplate. As shown in Figure 3-4, each bridge is composed of eight gages evenly spaced around the field side of the wheelplate at the same radius. The first four adjacent gages are placed in legs of the bridge that cause a positive bridge output for tensile strain and the next four gages are placed in legs causing a negative bridge output for tensile strain. The resulting bridge cancels out the strain due to the axial load because all eight gages are at the same radius with four causing positive and four causing negative bridge outputs. However, the bridge is very sensitive to the sinusoidal strain component associated with the hub moment due to the flange force because the tensile strains and the compressive strains above and below the axle are fully additive in bridge output twice each revolution (once as a positive peak and once as a negative peak). Radial gage locations may be chosen such that the bridge output varies sinusoidally with one cycle per wheel revolution. Two identical bridges 90° out of phase are used to obtain a force channel output independent of wheel rotational position as a consequence of the geometric identity:

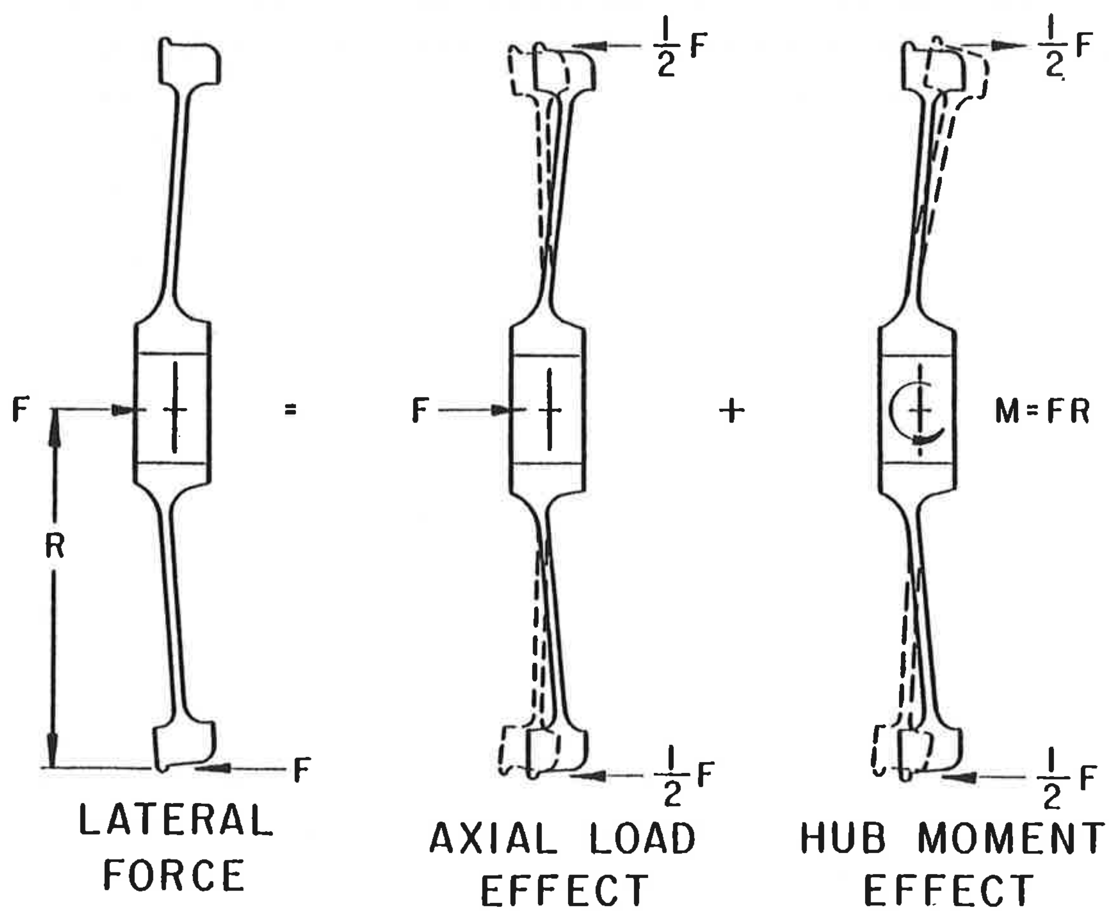

FIGURE 3-5. LATERAL FORCE STRAIN DISTRIBUTION

$$\sqrt{(L\sin\theta)^2 + (L\sin\{\theta+90^\circ\})^2} = |L| \text{ for any } \theta$$

3.2.2 PRIMARY SENSITIVITY AND CROSSTALK

The first step in the production of the instrumented wheels was the machining of both to an identical contour. The contour was dictated by the minimum allowable wheelplate thickness and by the production variation of the available sample of wheels. The machining contour is usually close to the original design shape but at a minimum thickness. The thinning of the wheelplate is the easiest step in maximizing sensitivity because it does not involve compromise with the other measurement properties of the wheel.

The most powerful tool in selecting the radial locations of the strain gages for the best compromise between primary sensitivity, crosstalk, ripple, and sensitivity to axial load point variation is a detailed empirical survey of the strains induced in the given wheelplate by the expected service loads. The use of wheels machined to an identical profile makes the empirical approach to wheelset instrumentation practical because the results of the strain survey may be applied to all wheels in the group. The calibration loads and the reference lateral position of the wheel on the rail should reflect the type of experiment in which the wheels will be used.

The WMATA car wheels were loaded both to the nominal static load of 10,000 lb and to 15,000 lb (to simulate load transfer) with the rail adjacent to the flange to determine the primary vertical sensitivity. Lateral loadings of 1,000 lbs., 2,000 lbs., 5,000 lbs. and 10,000 lbs. were made while maintaining the 15,000 lbs. vertical load. The normalized difference in lateral bridge strain between the highest combined load and the purely vertical load is the lateral sensitivity, and the other loads were taken to verify linearity. The combined vertical and lateral loading at a high L/V ratio accomplished by forcing the wheelset laterally against a rail while maintaining a vertical load was used to select strain gage locations for minimal crosstalk. Vertical loadings at several points across the tread were taken to evaluate the sensitivity to axial load point.

In the strain survey conducted on the WMATA car wheels, strain gages were applied at intervals of one inch or less on both field and gage sides of the wheelplate along two radial lines separated by 180° of wheel arc. The calibration loads were repeated at every 15° of wheel arc until the strain along 24 equally spaced radial lines on both gage and field side was mapped for each load. This data was used in a computer program to predict the output of a force channel as a function of the radial locations of the gages in the companion bridges.

The vertical force measuring bridges of the WMATA car wheels have strain gages on both sides of the wheelplate. The simulation program allowed the rapid trial of many combinations of gage and field side radii as potential strain gage locations. The maximum sensitivity possible for a purely vertical load on a given wheel of a bridge actually producing the triangular waveform is rapidly revealed. The "triangularity" of the waveform of a candidate bridge can be tested by adding its output at each angular load position to that at a load position advanced by 45° of wheel arc. This test determines the ripple expected of a force channel composed of two out of phase candidate bridges.

A lateral force affects the vertical bridge both by directly changing the strain pattern in the wheelplate and by moving the point of vertical load contact with the rail toward the flange. By using as a measurement of crosstalk the difference in bridge output caused by adding a lateral load to an existing vertical load, correction factors may be chosen which compensate for net lateral force crosstalk which includes direct lateral force crosstalk and the effect of slight vertical load point movement. It is desirable to identify vertical bridges in which the direct lateral force crosstalk and the effect of load point changes are opposed and yield a minimum net crosstalk for flange forces in service. The accuracy of the highly loaded flanged wheel is enhanced using a correction factor in processing based on the net lateral force crosstalk. Compromises in bridge selection are usually biased in favor of the flanged wheel because it generates the most vital data for vehicle dynamics or rail wear studies.

The primary sensitivities and crosstalk factors achieved for the WMATA car wheels are listed in Table 3-1. The vertical bridges were chosen from a detailed simulation with radial position increments of 0.1 inches on the basis of maximum primary sensitivity while holding the simulated ripple below 5% and minimizing crosstalk and sensitivity to axial load point. The primary sensitivity was observed to be linear within about 1% because the strains at each gage are low and the wheelplate behaves elastically. Primary vertical force sensitivity appears to be inversely proportional to tread diameter and wheelplate thickness for several wheelplate shapes which have been instrumented by ENSCO.

The lateral force measuring bridges of the WMATA car wheels have gages on only one side of the wheelplate and the trial simulation of bridges is used to determine the most advantagous side of the wheel and the radial gage position. Sensitivity was measured with combined vertical and lateral loads and crosstalk was determined from purely vertical loads. A very high sensitivity was achieved for good resolution, but at low lateral forces the linearity also required special consideration. The lateral force is computed from the sum of the squares of two bridge outputs causing all measurements to have a positive sign. The convenient determination of the direction of a lateral creep force requires

TABLE 3-1. CHARACTERISTICS OF WMATA CAR INSTRUMENTED WHEELS

A. Calibration Constants

Wheel Description	Vertical Force Measurement: Sensitivty	K	Raw Lateral Force Crosstalk*	Lateral Force Measurement: Sensitivity	Raw Vertical Force Crosstalk*
28" tread dia.; convex conical wheel plate, 3/4" min. thickness	7½ $\mu\varepsilon$/kip	.95	10-20%	60 $\mu\varepsilon$/kip	7-17%

B. Uncorrected Variability

Vertical Force Measurement: Sensitivity to Axial Load Point	Max.Ripple Vertical Load	Max.Ripple Combined Load	Lateral Force Measurement: Sensitivity to Axial Point	Max. Ripple Combined Load
+10%/inch	±5%	±7%	-3%/inch	±3%

*Crosstalk varies with tread taper; the force indication is entirely compensated for crosstlak by the wheel processor.

a wheel rotational position sensor. (It can also be accomplished by careful examination of the sinusoidal output of a single bridge.) It is possible that a purely vertical load can cause a lateral bridge output having a sign opposite to that caused by lateral force, but the crosstalk would appear positive because of squaring. The first increment of lateral load would cause a reduction rather that an increase in the output of such a bridge and bridge strains at low lateral forces would not be unique to a particular force. Although this would be of little concern in an experiment to measure high L/V ratios, low force measurements were vital to this test program. It is more important to optimize the sign of the vertical crosstalk than its magnitude where the lateral force measurement range extends to low forces. Raw vertical into lateral crosstalk of up to 17% (varying with taper) rather than the usual 1-3% was a consequence of optimizing the vital properties, but the processor compensation completely removed the crosstalk from the force indication.

3.2.3 RIPPLE

Ripple is caused by the failure of the bridges to produce the desired waveform and by deviation from the correct phase relationship between the companion bridges which are processed together as a force channel. The wheelplates are machined for uniformity to reduce ripple and a grid of radial and circumferential lines is scribed on the wheelplate to aid accurate gage placement. The massive computer aided simulation of trial bridges was used to determine gage locations of minimum inherent ripple. The ripple of the vertical force channel is reduced by attenuating the high bridge sums occurring between the rounded bridge peaks as shown in Figure 3-4. This method achieves a substantial reduction in ripple at a small cost in average sensitivity.

The lateral bridge output is inherently very sinusoidal. The requirement for two bridges at the same radius out of phase by 90° is in conflict with the 45° spacing between the gages in each bridge because theoretically both bridges should occupy the same space. Placing the gages side by side causes a deviation from the proper phase relationship which manifests itself as a ripple. Table 3-1 gives the maximum ripple for the WMATA car wheels. Larger wheels which have less phase deviation between lateral bridges also have less ripple. Greater ripple is measured at combined loads because crosstalk produces distortions of the waveforms.

Ripple does not create as much error as might be supposed. Even the peak wheel forces measured during vehicle dynamics testing frequently are averaged for about 50 milliseconds. A 28-inch wheel makes half a revolution in 50 milliseconds at 50 mph, substantially negating ripple in a 50 millisecond average wheel force since 2 cycles per revolution is a typical ripple frequency. A single instantaneous measurement is rarely sought and filtering has a mitigating influence on ripple similar to time averaging.

3.2.4 LOAD POINT SENSITIVITY

Lateral changes of the point on the tread where the wheel contacts the rail affect the bridge strains in two ways. The change in hub moment is similar to the effect of a lateral force. It acts directly on the lateral bridge and through crosstalk on the vertical bridge. However, the failure of the tread to transmit the moment due to load point offset uniformly into the wheelplate probably has the major effect on the vertical bridge. Unsymmetric changes in the local intense compressive strains in the wheelplate above the rail contact can influence the vertical bridge sensitivity. Wheels with thin tread hoops are most susceptable in this regard. The load point sensitivity of the WMATA car wheels (Table 3-1) remained stable despite several retaperings, indicating sufficient remaining tread hoop stiffness.

The effect of load point sensitivity on measurements taken with the WMATA car wheels on the high rail was negligible because the calibration was performed with the wheel flange adjacent to an actual rail. The true vertical load on the unflanged low rail wheel is about 15% less than the indicated. To correct the lateral force indication of the unflanged low rail wheel, its absolute value should be increased by about 5% of the corrected vertical if it is zero or positive (toward the flange) or decreased by the same amount if it is negative.

$\sqrt{\sin^2 + \cos^2}$ TECHNIQUE (EMD)

- TWO BRIDGES
- SINUSOIDAL OUTPUT
- 90° OUT OF-PHASE
- APPLIED AT SINGLE RADIUS TO ONE SIDE OF WHEELPLATE

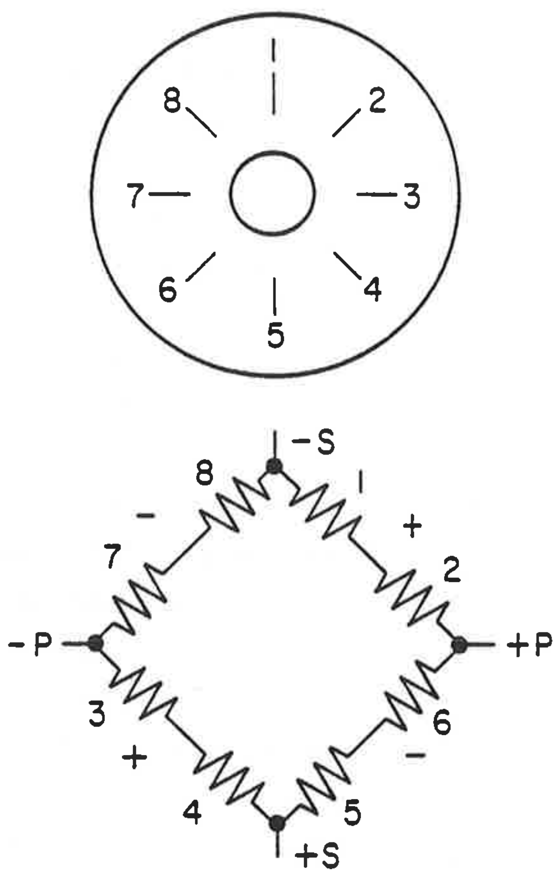

GAGE LAYOUT

BRIDGE WIRING

FIGURE 3-6. LATERAL FORCE MEASUREMENT BRIDGE

3.2.5 THERMAL AND CENTRIFUGAL EFFECTS AND OTHER SOURCES OF DRIFT

The vertical and lateral bridges used on the WMATA car wheelsets are particularly immune to drift by virtue of strain gage location and instrumentation technique. Strains induced by thermal change and centrifugal force are radially symmetric on each side of the wheelplate. The lateral bridge consists of eight gages at the same radius on the same side of the wheelplate positioned in the bridge so that four add and four subtract. A radially symmetric strain field is cancelled by the additions and subtractions. Similarly, the vertical bridges have four gages at the same radius on each side of the wheelplate. On each side two gages add and two subtract.

Each bridge generates a triangular or sinusoidal waveform as the wheel rotates under load. High pass filtering of the amplified bridge signals at 0.2 Hz does not attenuate the oscillating part of the signal but it forces the signal to oscillate about zero. High pass filtering eliminates gradual drift that could occur from thermal effects on the wheelset wiring and wheel to amplifier cabling and zero drift of the strain gage bridge amplifiers. It would also suppress thermal and centrifugal effects in bridges which do not self cancel them.

3.2.6 SENSITIVITY TO LONGITUDINAL FORCE

Longitudinal forces involved in braking and driving are extraneous influences on the vertical and lateral force measurement bridges. Brakes on instrumented wheelsets are usually disabled to avoid sensor damage by overheating and to avoid accidental flatspotting. However, instrumented wheelsets on self propelled vehicles must cope with driving forces. Figure 3-7 shows the strain distribution in a driven wheel. The longitudinal force may be resolved into a torque about the axle and a horizontal force perpendicular to the axle. The similarity between this horizontal force component and the vertical force suggests an error source.

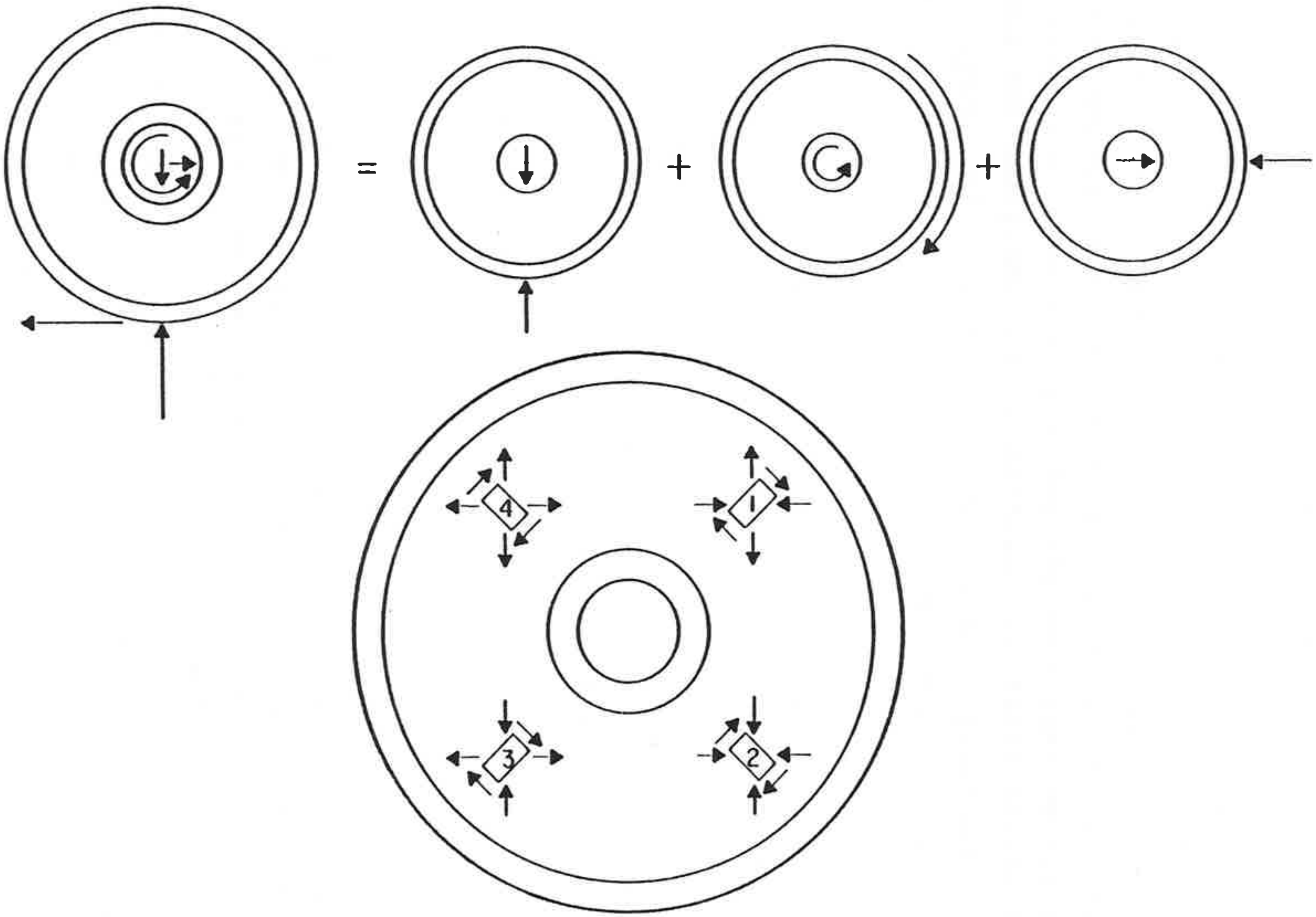

FIGURE 3-7. LONGITUDINAL FORCE STRAIN DISTRIBUTION

The vertical force measuring bridges on the WMATA car wheelsets are configured in such a way as to cancel the effect of longitudinal forces. Figure 3-7 shows the strain components at four gage positions on one side of the wheelplate due to vertical and driving forces. The bridge is shown in the vertical null output position. Gages at 180^o spacing add together in their contribution to the bridge summation. The vertical, horizontal and shear components of strain are opposite in sense for gages spaced 180^o apart and cancel each other out retaining the null bridge output. The longitudinal force does not create an intense local strain aligned with the sensitive axis of a strain gage which stimulates the vertical bridge in any rotational position. The insensitivity of the vertical bridges to longitudinal force has also been verified experimentally.

The lateral bridges used on the WMATA car wheels are also insensitive to longitudinal forces. The symmetric gage pattern limits the effect of the shear strains, but the horizontal force has the effect of adding vectorially to the vertical force to produce crosstalk. Since the longitudinal force is limited by friction to about 1/4 the vertical load, the vector sum of forces is only about 3% higher than the vertical force alone. An increase in crosstalk of 3% of 12% and (0.36%) is insignificant.

3.3 DATA ACQUISITION SYSTEM

Figure 3-8 is a block diagram of the data acquisition system.

The displacement and acceleration sensors described in the previous sections were cabled to junction boxes containing power supplies and to signal conditioning amplifiers where the full scale range of ± 10 Vdc was established. The outputs of the speed, traction motor current and location detection sensors were also scaled by the signal conditioning amplifiers.

The instrumented wheel strain gage bridge circuits were connected to the strain gage amplifiers by means of rotating sliprings at

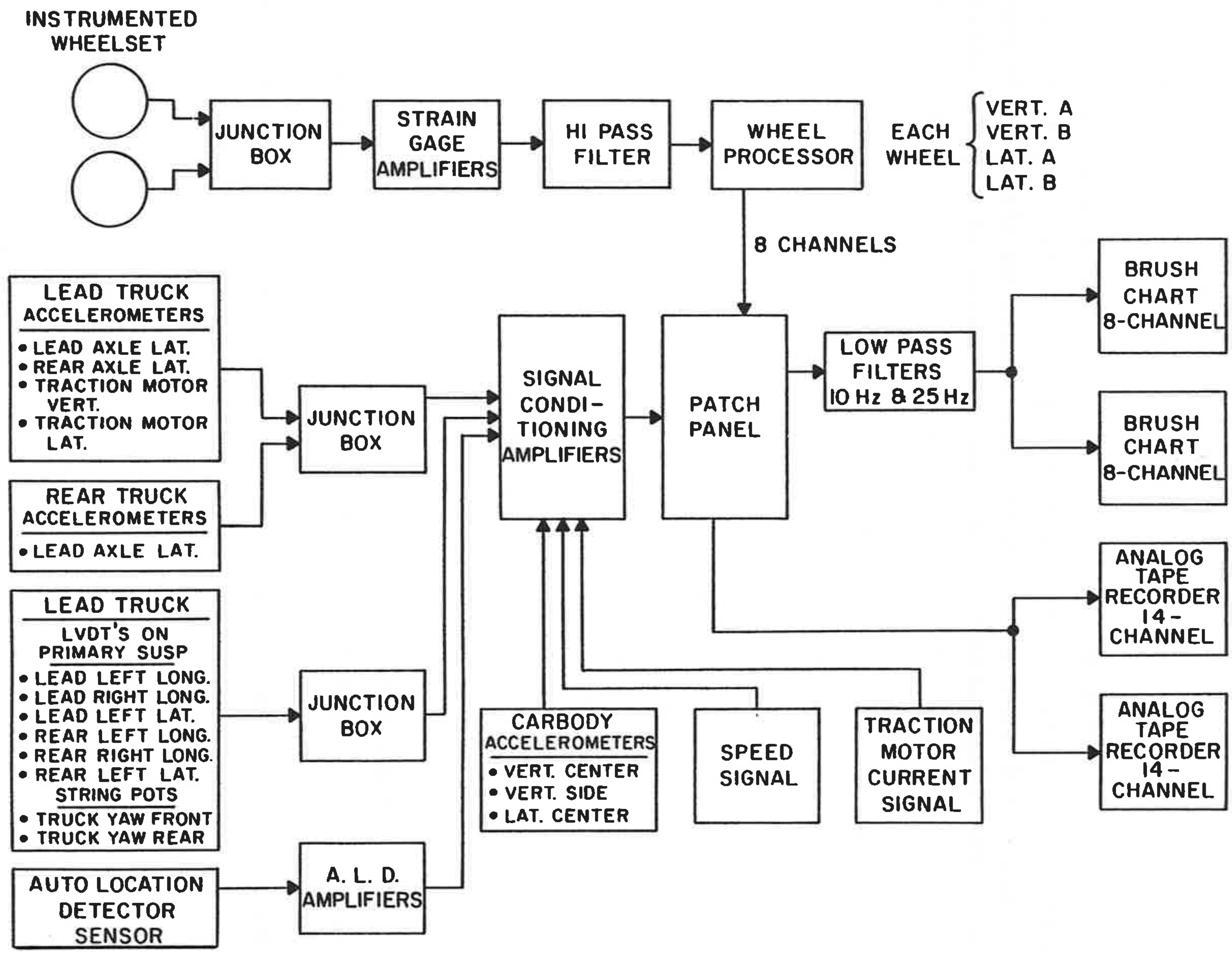

FIGURE 3-8. DATA ACQUISITION SYSTEM

each end of the axle and a junction box to join the wheel cables. The strain gage ammplifiers supply ac carrier excitation to the bridges and demodulate the bridge responses to produce highly amplified dc signals proportional to the bridge strain summation. Carrier amplifiers provide superior noise immunity.

As the wheels rotate, the output of the individual bridges (two bridges are required for each force channel) under a constant force vary as sine waves or triangular waves. High pass filtering is applied to the rotating wheel bridge output to eliminate all sources of signal drift. Wheel rotation causes the bridge responses to oscillate at the wheel rotation frequency with drift resembling a change in dc level. High pass filtering strikes out the drift while preserving the ac waveform thus eliminating the need for rezeroing even during long test days.

The wheelplate processor combines the individual bridge signals to form continuous force measurements. It also performs cross-talk correction and scaling to a ±10 Vdc range proportional to ±25,000 lb. wheel/rail force.

The wheelset outputs and the conditioned outputs of all the other sensors are merged at a patch panel. All of the signals were recorded by the analog tape recorders, but the patch panel allowed sampling of the various sensors for real time observation with the strip chart recorders. The data signals were filtered before observation on the strip charts, but they were recorded on magnetic tape at the frequency response of the sensors.

3.4 DATA REDUCTION

The data presented in Appendices A and B were obtained by reading strip chart recordings. The data tapes were replayed to the strip chart recorders after the test was finished so that attention could be given to holding accurate zeros. The accelerometer channels were filtered at 10 Hz and the force and displacement channels were filtered at 25 Hz.

The steady state readings were averaged by inspection over the length of the constant radius part of each curve. The constant radius part of the curve was identified by targets placed on the ties for detection by the ALD sensor and by the character of the high rail lateral force indication.

The peak readings were simply the highest filtered level attained at the spirals or body of each curve. The filtering was used to elminate events having such short time duration that they were insignificant to the dynamic behavior of the vehicle.

A second type of peak indication was also listed in the stability test data included in Appendix B. It was the level exceeded for a time of 100 milliseconds. It was used to eliminate more events on the basis of time duration to make hunting, should it occur, more obvious against the background of ordinary rail roughness.

4.0 TEST RESULTS

The principal data channels appropriate for each type of test run have been reduced and are tabulated in Appendix B. Auxilliary data channels have not yet been reduced except for isolated runs to check for consistency. The peak and steady state lead wheel lateral forces at each test curve have been plotted versus vehicle speed in Appendix A. A detailed analysis of the test results is presented in Part I of this report, and only a few general observations are offered below.

4.1 CURVING

Figure 4-1 summarizes the steady state lateral force mesurements by plotting the data (interpolated to balance speed) versus curve radius for combinations of suspension bushing stiffness and wheel taper (1:20 and cylindrical). Both changing from stiff to soft bushings and changing from cylindrical to tapererd wheels produced consistent reductions in flanging forces. Suspension compliance appeared to be the more effective change at sharp curves of less than 1000 ft. radius, and wheel taper was the more beneficial change at curves of larger radius.

The combination of changes was especially effective. Reductions of lateral force between 60% and 90% were achieved, and the effect of the combined changes was greater than the sum of the effects of the individual changes.

Curve 311 was the only right curve of the six test curves. Measurements of truck geometry indicated a slight skewing of the axles that could bias it against curving to the right, and this bias may account for the high force measurements at curve 311. The combination of soft bushings and wheel taper appeared to reduce the sensitivity of the truck to production variations.

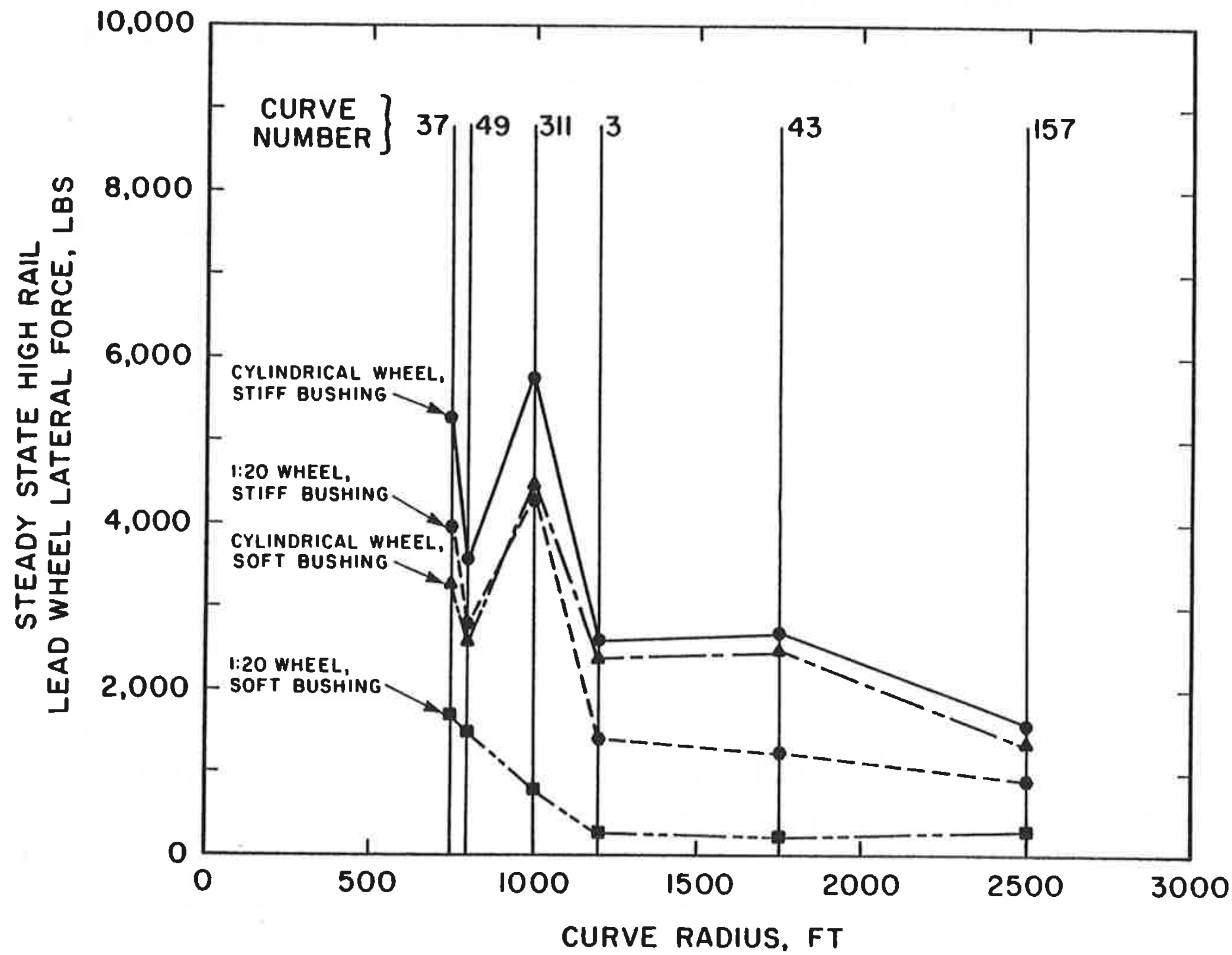

FIGURE 4-1. SUMMARY OF STEADY STATE LATERAL WHEEL FORCES ON THE HIGH RAIL AT BALANCE SPEED

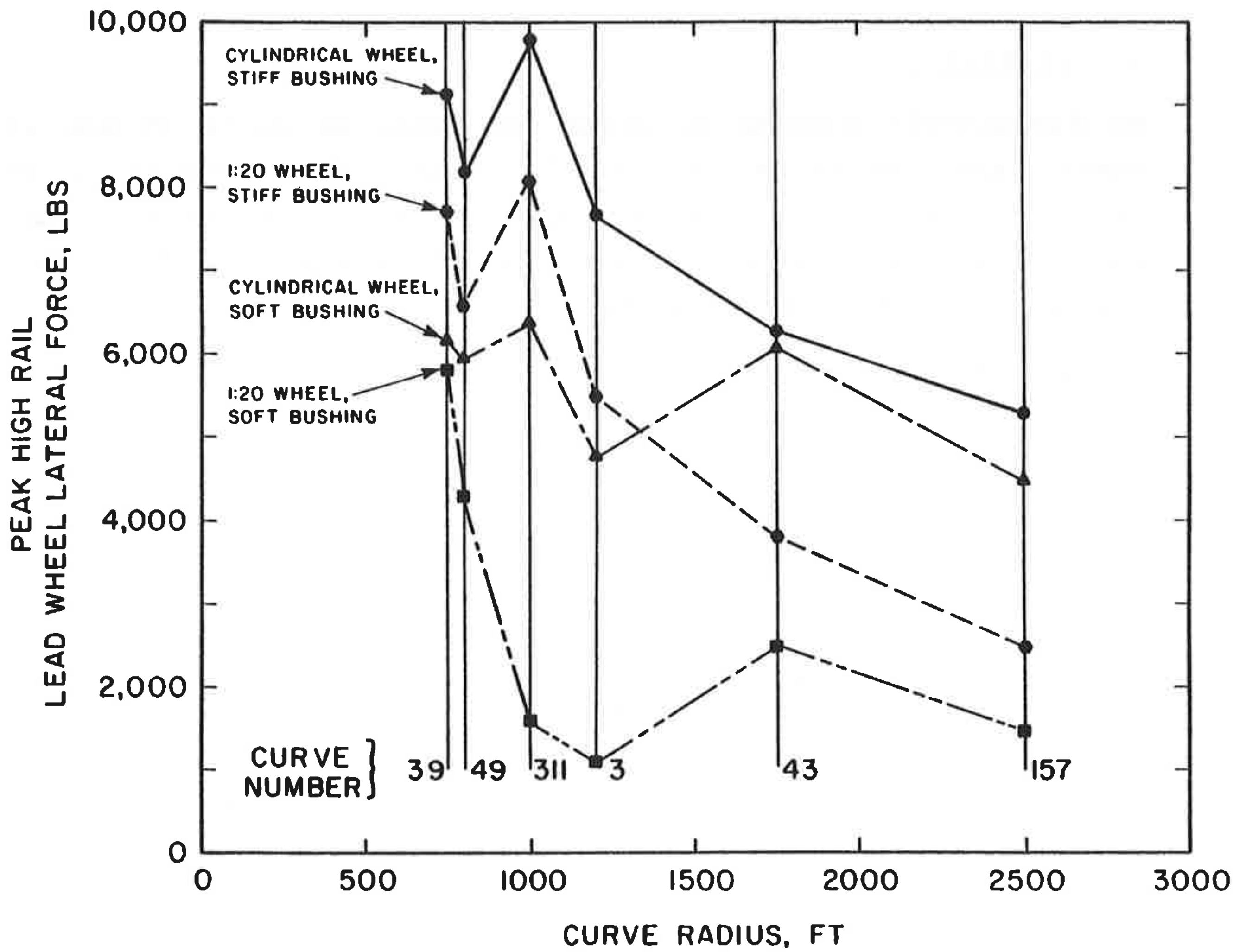

FIGURE 4-2. SUMMARY OF PEAK LATERAL WHEEL FORCES ON THE HIGH RAIL AT BALANCE SPEED

The same observations can be made for the peak measurements presented similarly in Figure 4-2. The change to greater longitudinal suspension compliance seemed the more effective for curves up to about 1300 ft. radius, but the combination of changes was extremely effective in reducing peak lateral flange forces in all cases.

4.2 STABILITY

No discernable hunting occurred for tests at up to 75 mph with wheel taper as great as 1:10 for either the standard or soft longitudinal bushing. The attempt to test a greater wheel taper was frustrated because of inability of highly tapered wheels to negotate switch frogs smoothly.

APPENDIX A: STEADY-STATE AND PEAK LATERAL WHEEL FORCES ON THE HIGH RAIL VS. TEST SPEED DATA PLOTS

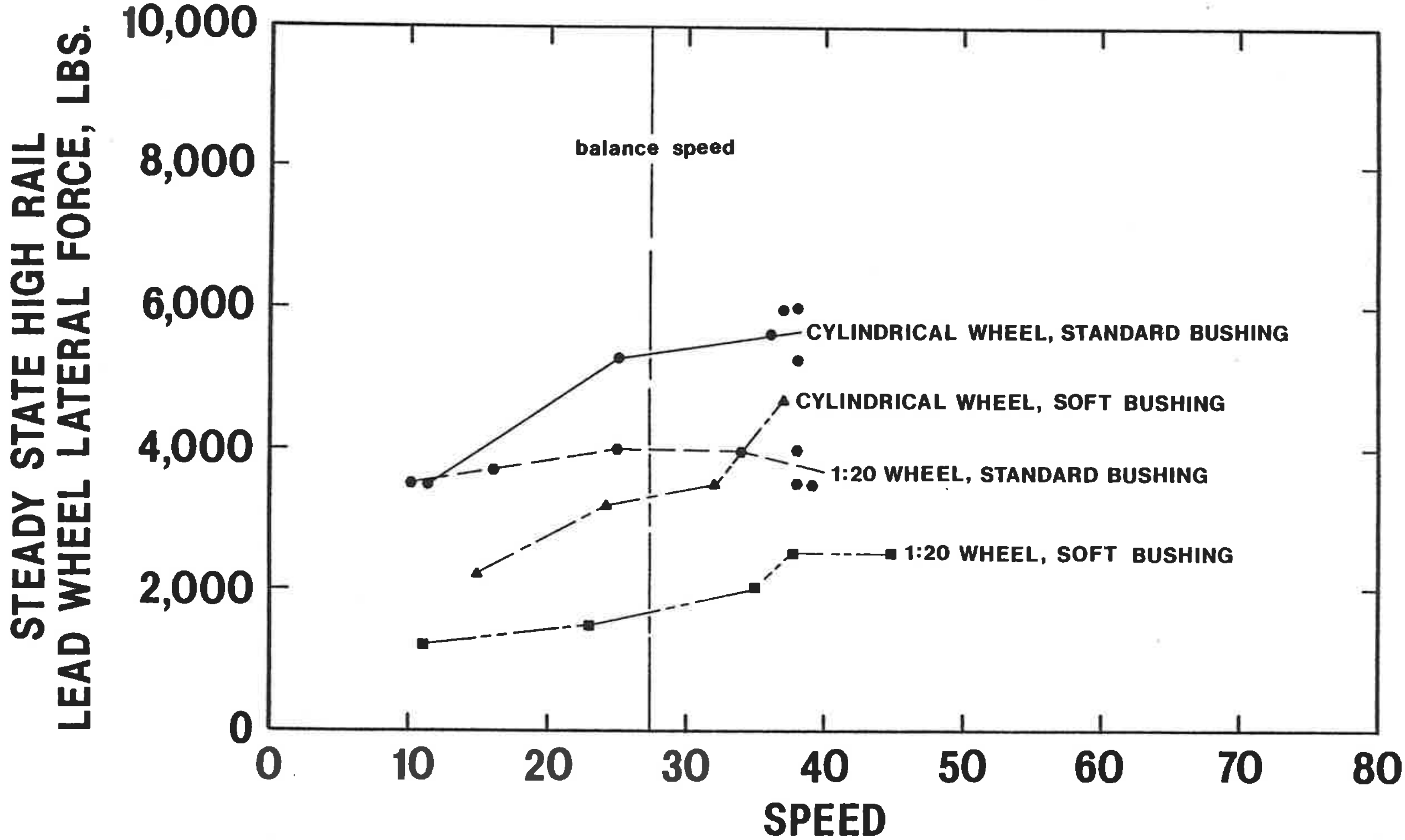

FIGURE A-1. CURVE 37 STEADY STATE LATERAL WHEEL FORCES

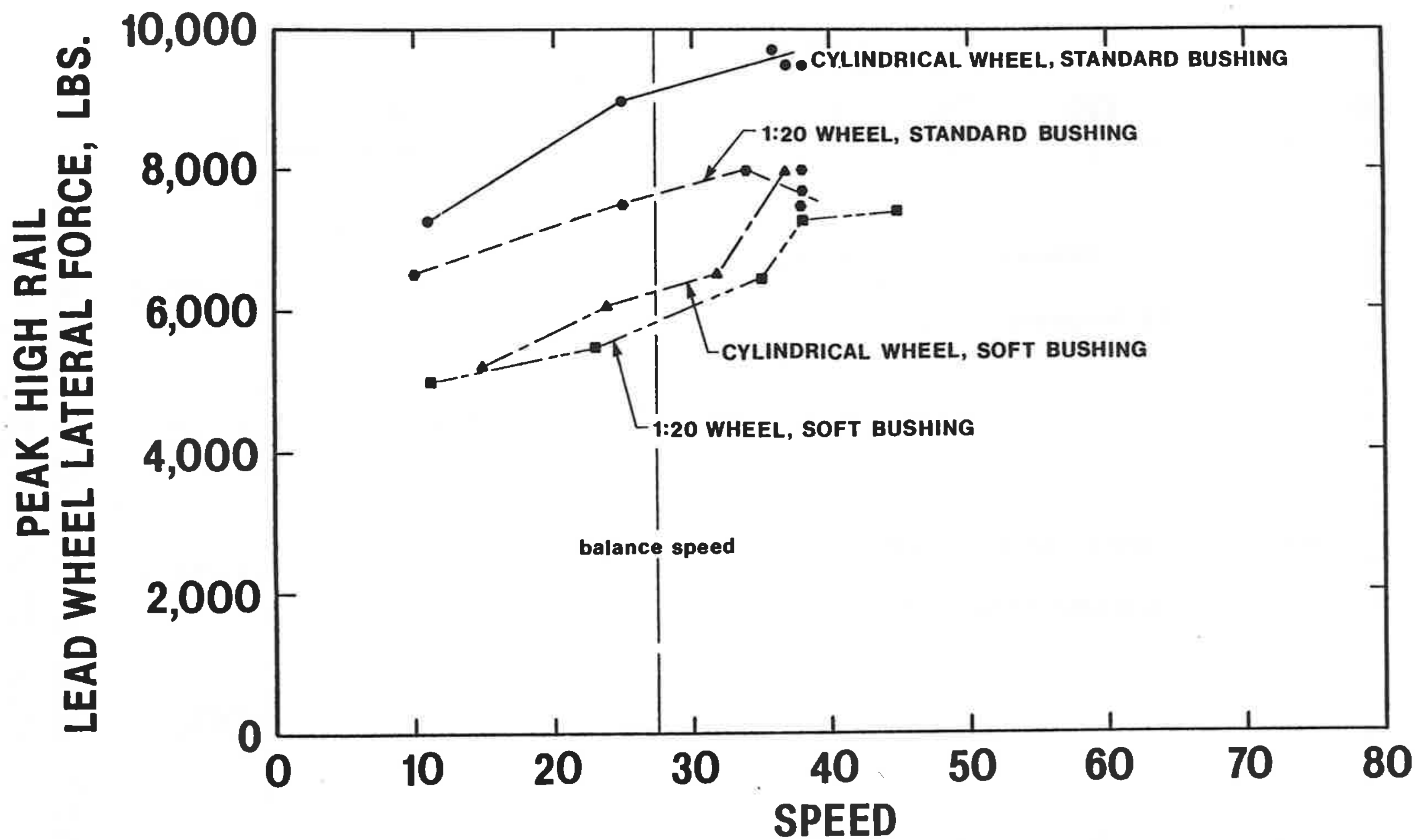

FIGURE A-2. CURVE 37 PEAK LATERAL WHEEL FORCES

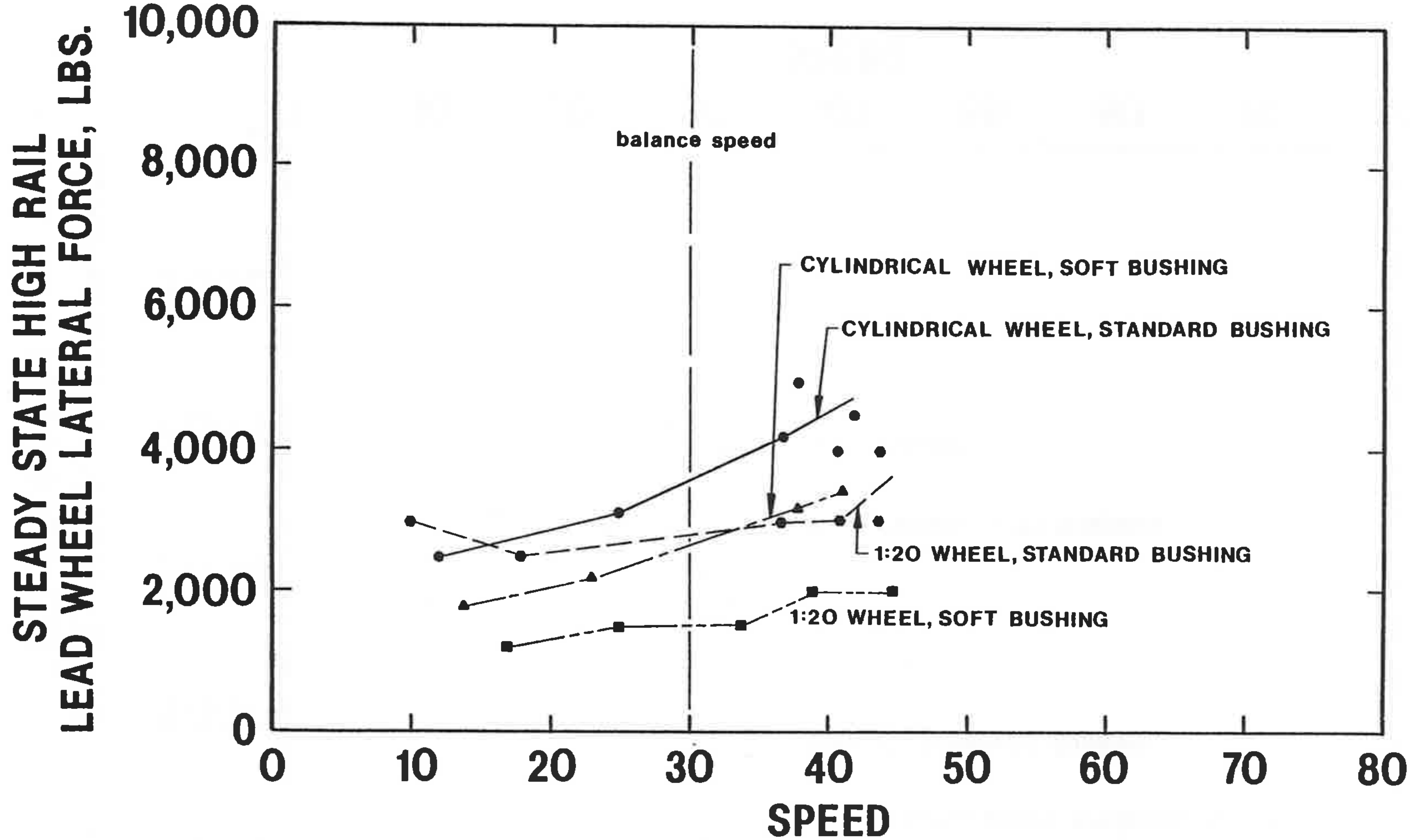

FIGURE A-3. CURVE 49 STEADY STATE LATERAL WHEEL FORCES

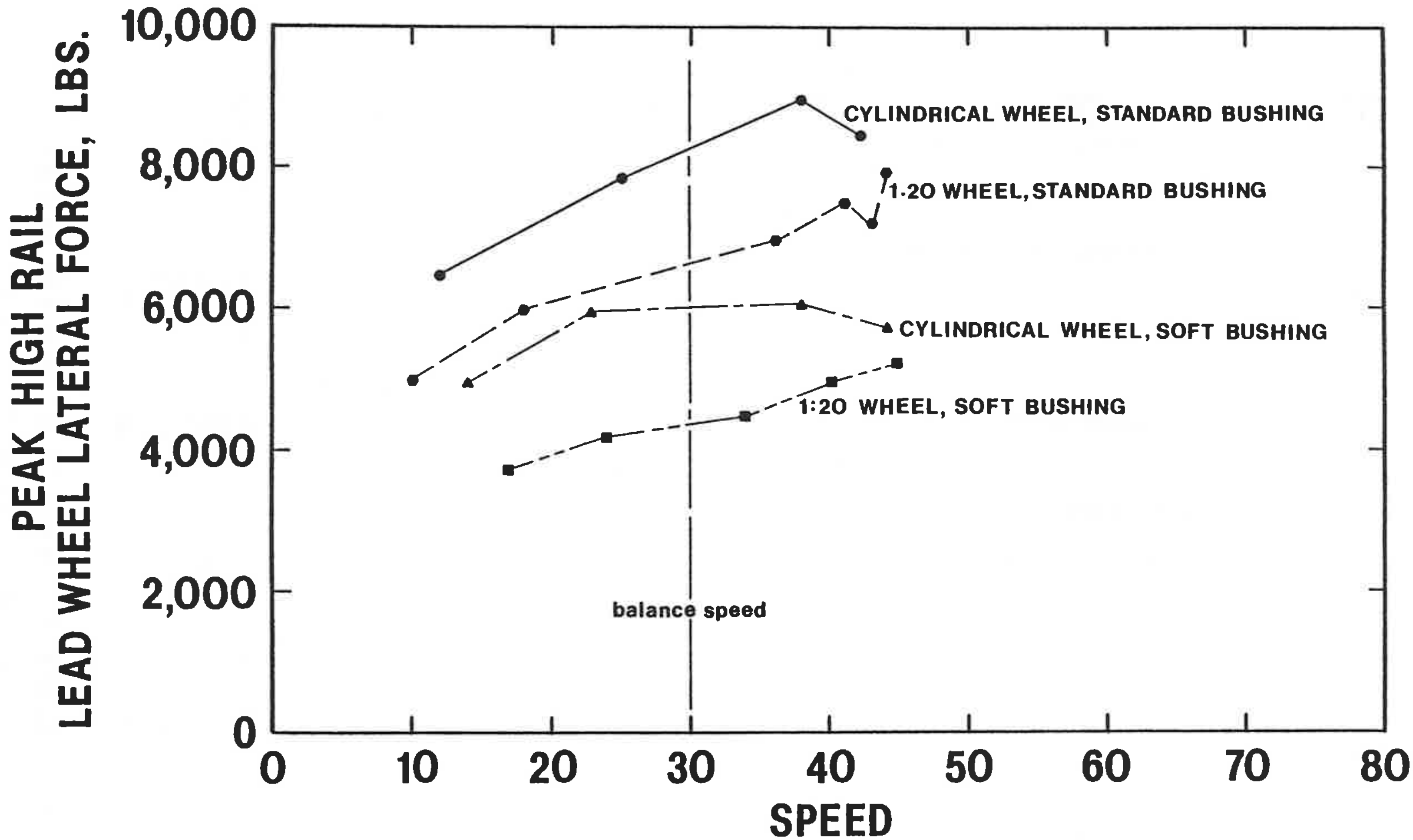

FIGURE A-4. CURVE 49 PEAK LATERAL WHEEL FORCES

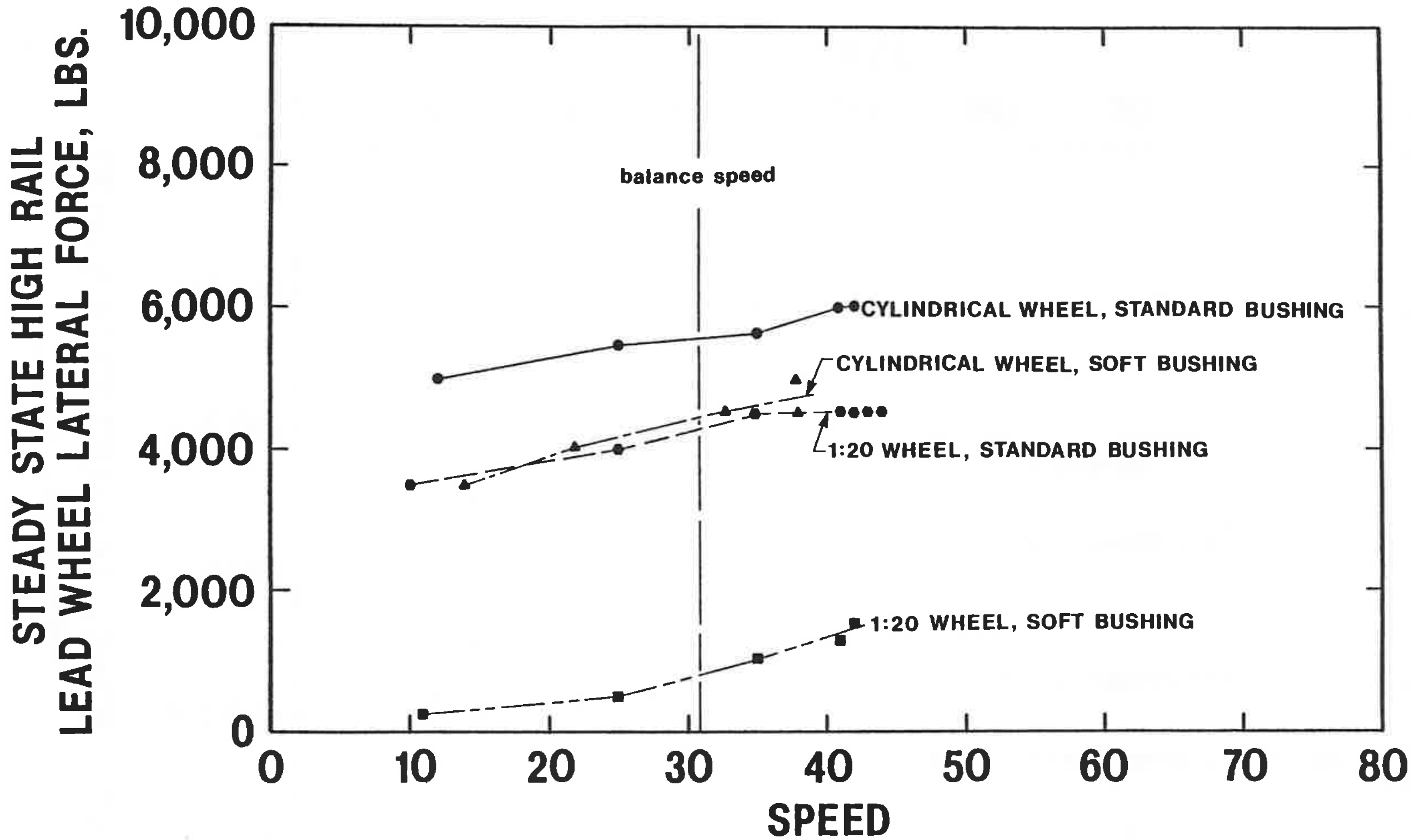

FIGURE A-5. CURVE 311 STEADY STATE LATERAL WHEEL FORCES

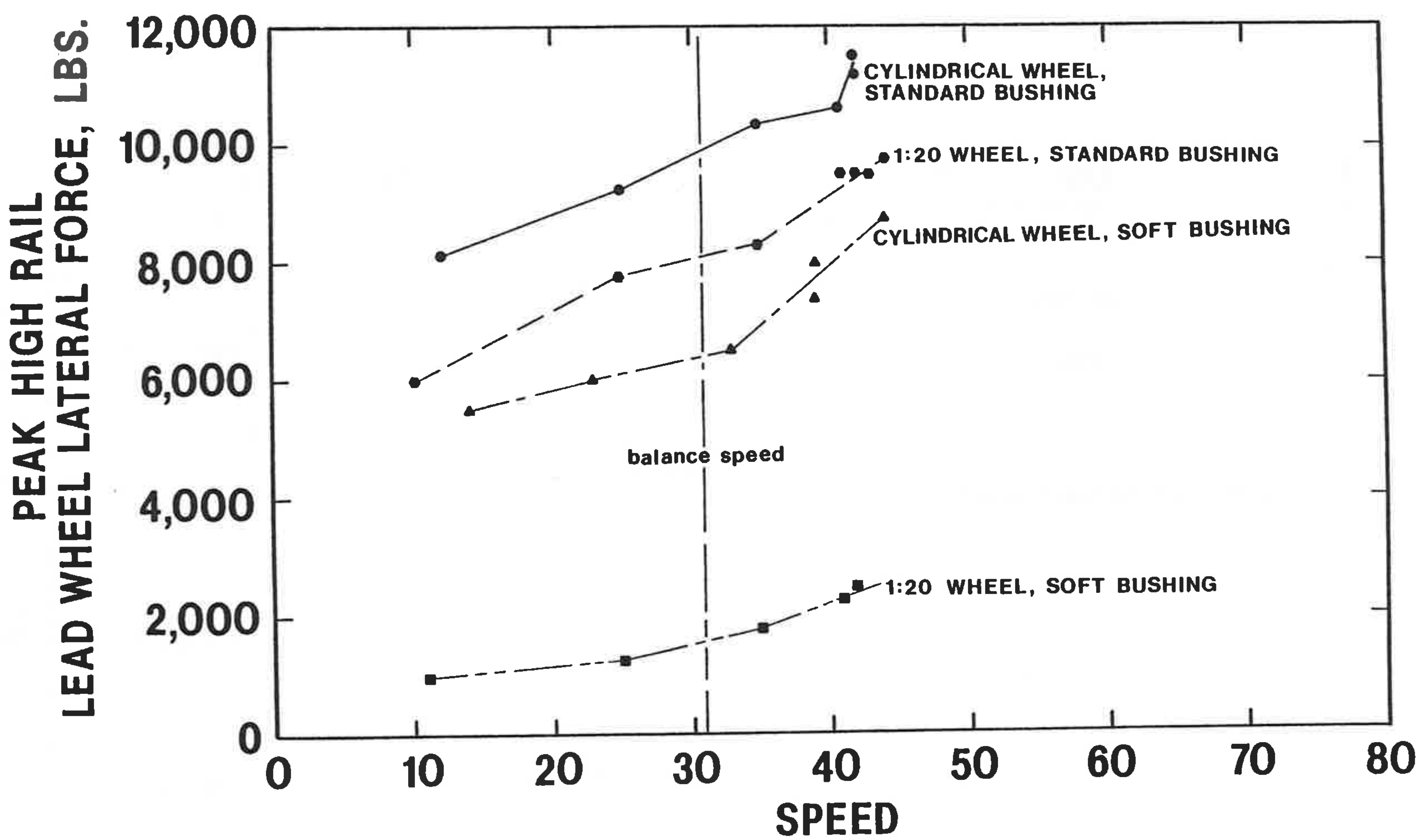

FIGURE A-6. CURVE 311 PEAK LATERAL WHEEL FORCES

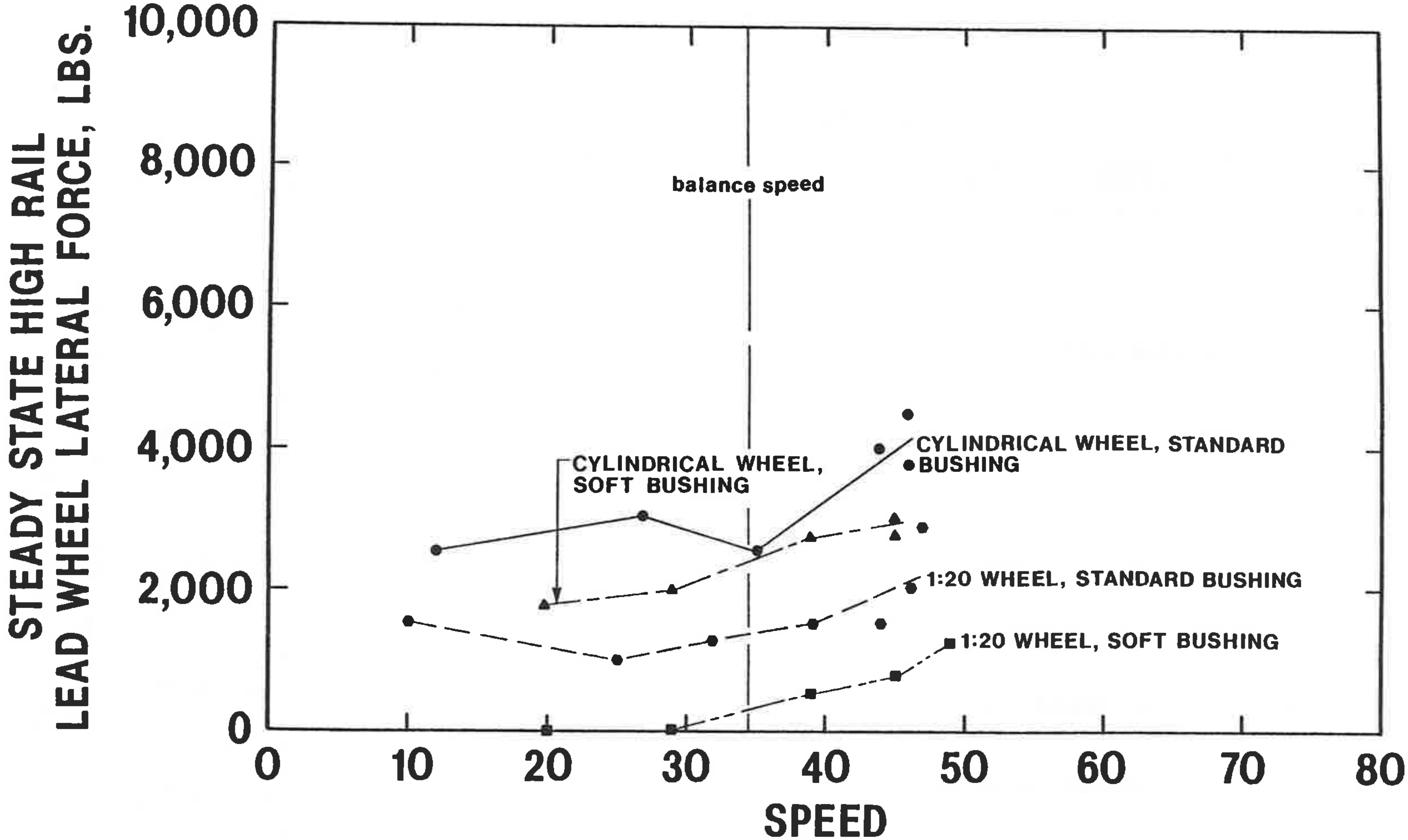

FIGURE A-7. CURVE 3 STEADY STATE LATERAL WHEEL FORCES

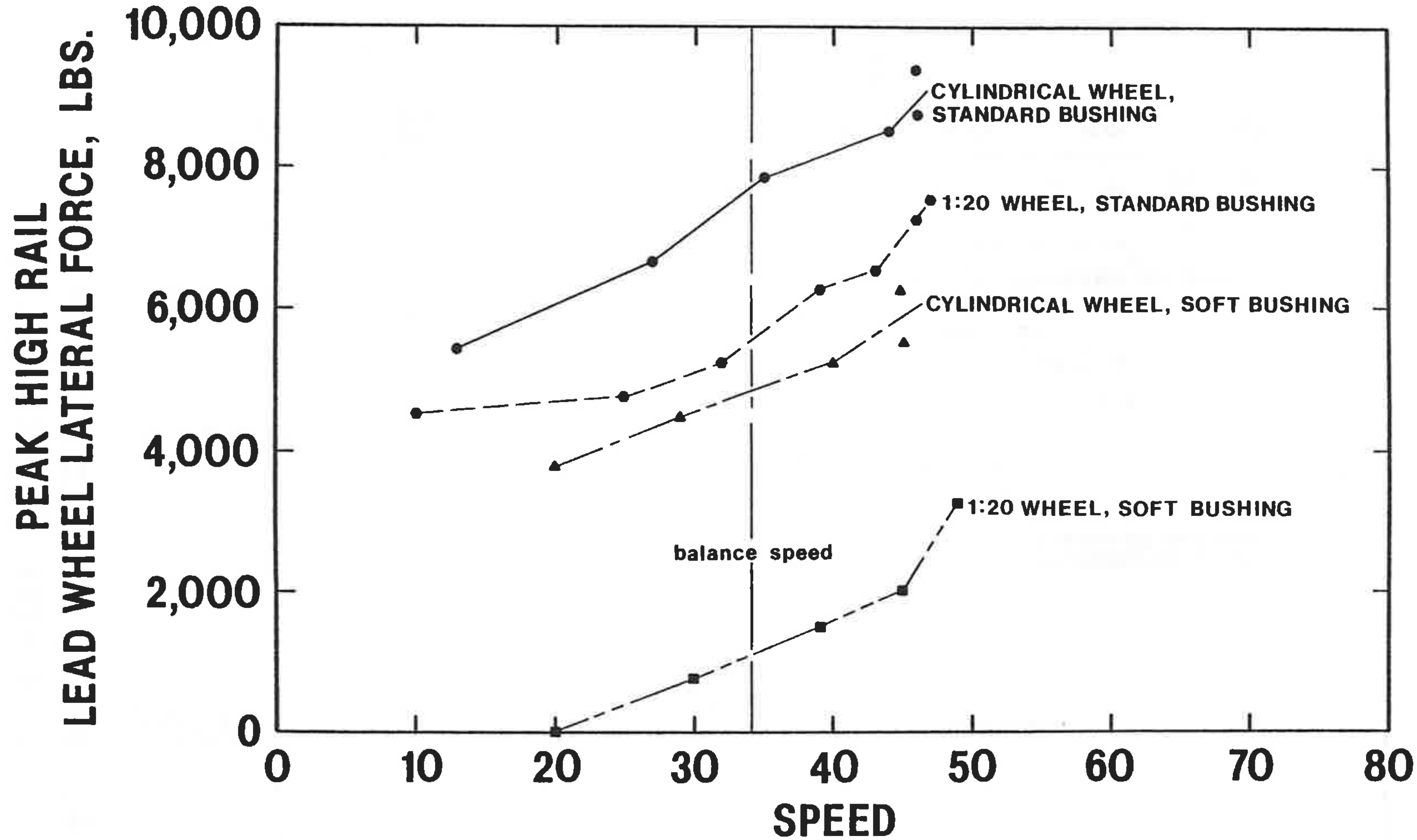

FIGURE A-8. CURVE 3 PEAK LATERAL WHEEL FORCES

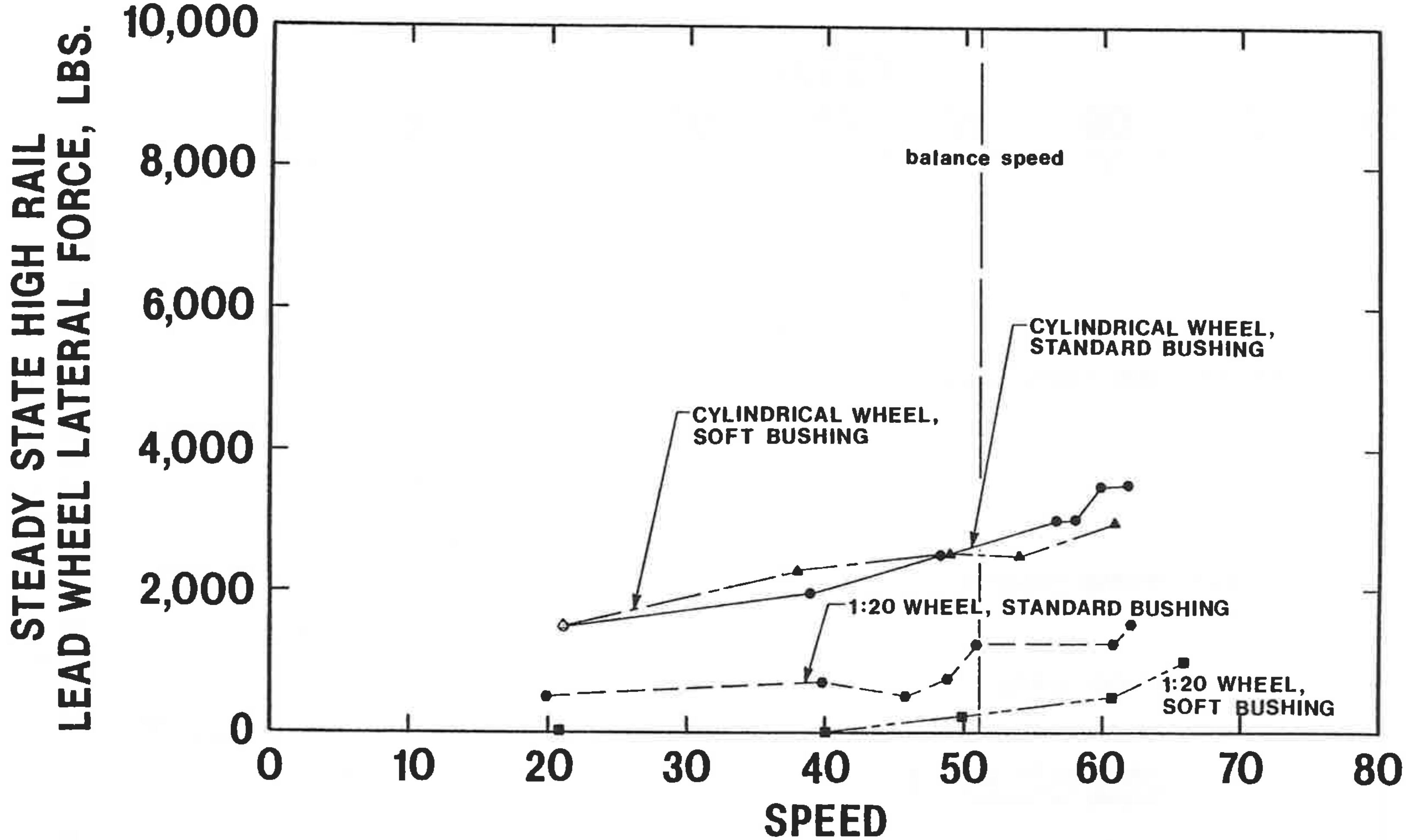

FIGURE A-9. CURVE 43 STEADY STATE LATERAL WHEEL FORCES

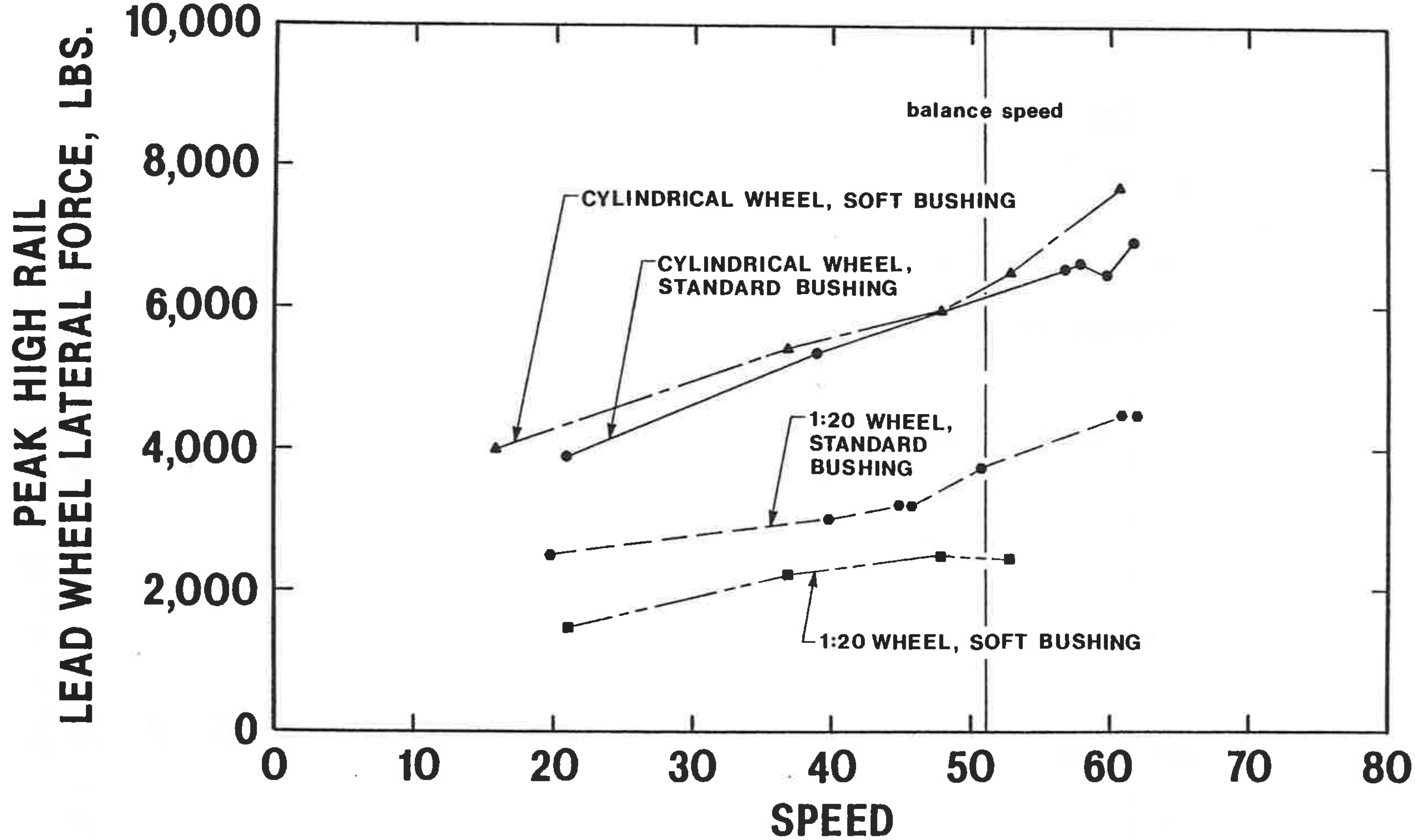

FIGURE A-10. CURVE 43 PEAK LATERAL WHEEL FORCES

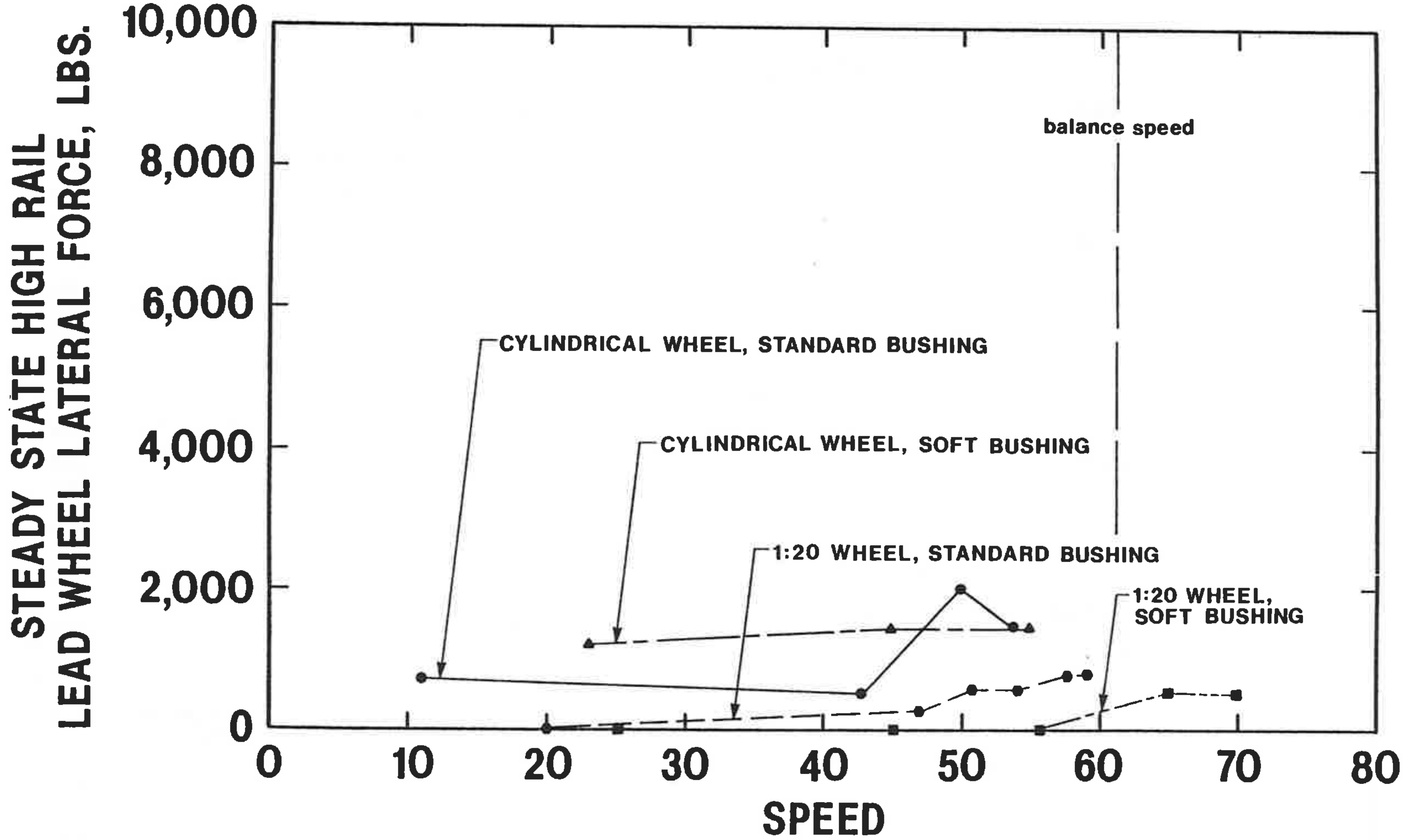

FIGURE A-11. CURVE 157 STEADY STATE LATERAL WHEEL FORCES

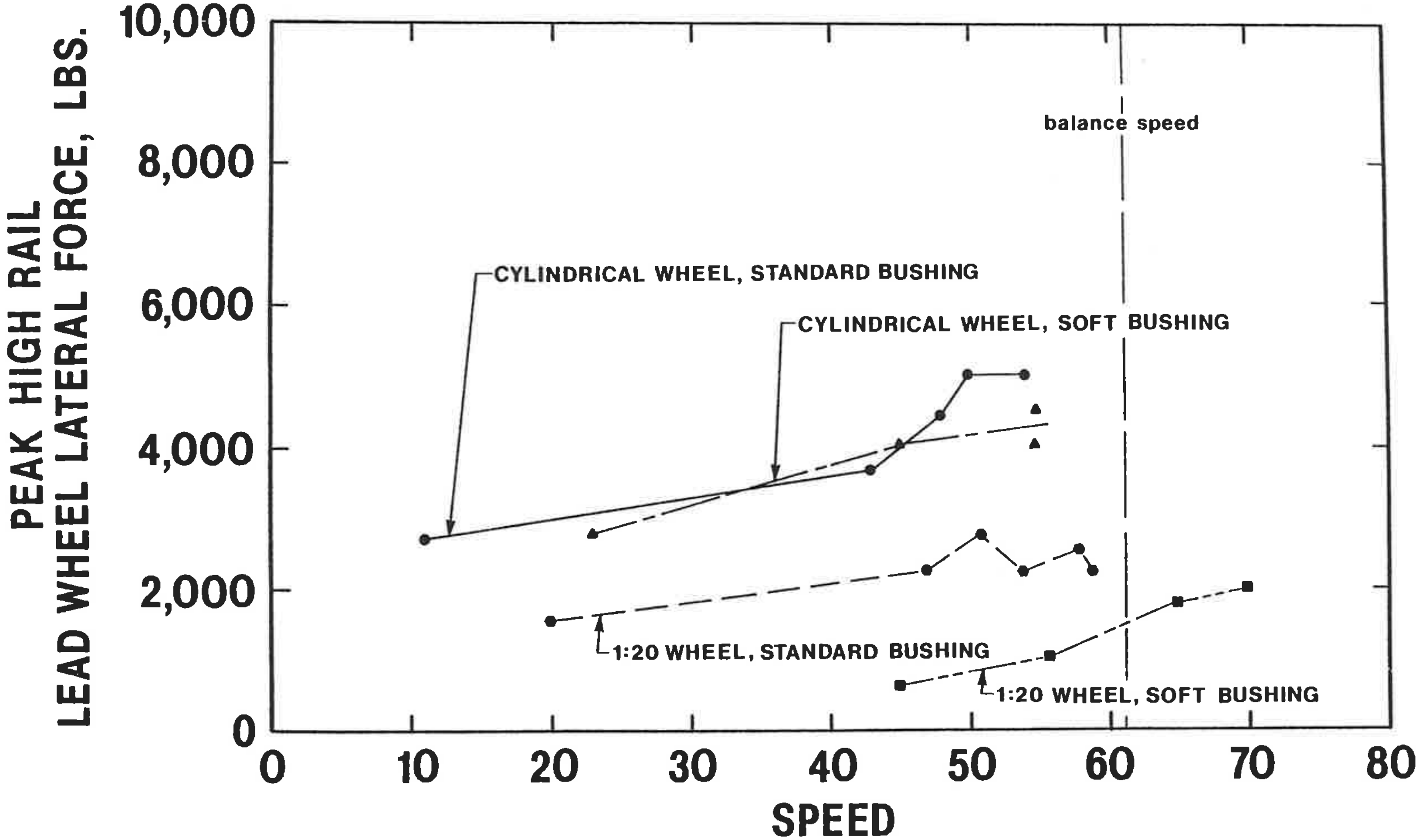

FIGURE A-12. CURVE 157 PEAK LATERAL WHEEL FORCES

APPENDIX B: TABULATED RESULTS BY TEST SERIES

LEGEND OF DATA ABBREVIATIONS

A. **RUN CODING**

example: 25 - G - SC (1R)

Day of the month

Test Series

A - cyl; stiff
B - 1:20; stiff
C - 1:10, stiff
F - 1:10; soft
G - 1:20, soft
I - 1:20, stiff
J - cyl; soft

Test Type

SC - steady curving
RE - route evaluation
ST - stability
TR - acceleration in curve

Sequence Number

1 is the first run of a test type
2 is the second run of a test type
3 ...

Direction

R is reverse run
F or blank is forward run
(instrumented wheelset leading consist)

B. **MEASUREMENTS**

L_L - Left wheel lateral force, lbs.

L_R - Right wheel lateral force, lbs.

ΔY_{LF} - Front axle primary lateral displacement, measured at left, in.

ΔY_{RR} - Rear axle primary lateral displacement, measured at right, in.

ΔX_{LF} - Left front primary longitudinal displacement, in.

ΔX_{RF} - Right front primary longitudinal displacement, in.

ΔX_{LR} - Left rear primary longitudinal displacement, in.

$a_y A-1$ - Lateral acceleration; lead axle, lead truck, g's

$a_y A-2$ - Lateral acceleration; trailing axle, lead truck, g's

$a_y A-3$ - Lateral acceleration; lead axle, trailing truck, g's

SERIES A - STEADY CURVING, FORWARD

	Curve Number	SPEED Peak	SPEED S.S.	ΔL_L Peak	ΔL_L S.S.	ΔL_R Peak	ΔL_R S.S.	ΔY_{LF} Peak	ΔY_{LF} S.S.	ΔY_{RR} Peak	ΔY_{RR} S.S.	ΔX_{LF} Peak	ΔX_{LF} S.S.	ΔX_{LR} Peak	ΔX_{LR} S.S.
22 ASC(1)	3	13	12	2750	1500	5400	2500	-.016	-.004	-.017	-.008	-.044	-.029	-.031	-.025
22 ASC(2)		32	27	2950	1475	6650	3000	-.014	.001	-.018	-.004	-.047	-.030	-.040	-.026
22 ASC(3)		44	35	2150	900	7850	2000	.015	.001	-.023	-.007	-.050	-.038	-.029	-.020
22 ASC(4)		47	46	1400	750	8750	3750	.016	.004	-.020	-.008	-.040	-.030	-.042	-.030
22 ASC(5)															
22 ASC(1)	311	12	11	8150	5000	4750	3650	.025	.013	.015	.004	.041	.035	.056	.049
22 ASC(2)		25	24	9200	5475	4950	3800	.033	.011	.014	.003	.035	.028	.046	.039
22 ASC(3)		36	33	10400	5650	4700	3500	.030	.009	.017	.006	.033	.026	.047	.042
22 ASC(4)		42	40.5	10600	6000	3900	3000	.035	.009	.015	.006	.029	.022	.027	.023
22 ASC(5)															
22 ASC(1)	37	12	10	4450	3000	7250	4500	-.019	-.007	-.023	-.015	-.047	-.042	-.050	-.045
22 ASC(2)		25	24	3950	3000	9000	5300	.017	.005	-.023	-.009	-.044	-.036	-.052	-.045
22 ASC(3)		39	34	3600	2475	9750	4575	.021	.007	-.024	-.006	-.054	-.043	-.056	-.048
22 ASC(4)		39	37	3150	2000	9500	5250	.019	.007	-.023	-.008	-.047	-.039	-.049	-.044
22 ASC(5)															
22 ASC(1)	43	21	20	3100	1550	3850	1500	-.015	-.004	-.007	.001	-.045	-.028	-.023	-.015
22 ASC(2)		40	38	2975	1500	5400	2000	-.023	-.001	-.017	-.001	-.035	-.016	-.027	-.018
22 ASC(3)		57	56	2575	1100	6600	3000	.013	.004	-.017	-.003	-.047	-.025	-.024	-.014
22 ASC(4)		58	57.5	2450	1000	6650	3000	.013	.002	-.013	-.002	-.043	-.025	-.034	-.023
22 ASC(5)															
22 ASC(1)	49	13	11	3450	1550	6500	2600	-.015	-.001	-.014	-.004	-.049	-.037	-.040	-.031
22 ASC(2)		26	24	3650	1400	7900	3100	-.013	.003	-.019	-.008	-.038	-.024	-.036	-.019
22 ASC(3)		37	36	2100	900	6400	4250	.020	.007	-.015	-.007	-.047	-.031	-.028	-.020
22 ASC(4)		41.5	40	1900	850	6200	4000	.017	.009	-.013	-.003	-.038	-.029	-.025	-.016
22 ASC(5)															
22 ASC(1)	157	11	11	2450	1100	2750	750	-.022	-.009	-.014	-.006	-.028	-.008	-.019	-.009
22 ASC(2)		45	40	3800	870	3700	500	.019	.003	-.018	-.001	.016	.002	.014	.010
22 ASC(3)		56	52	2350	900	5000	1500	.015	.001	-.023	-.002	-.033	-.013	-.024	-.010
22 ASC(4)		52	44	2400	1150	4450	1600	-.015	.004	-.013	-.002	-.030	-.014	-.025	-.012
22 ASC(5)															

SERIES A - STEADY CURVING, REVERSE

	Curve Number	SPEED Peak	SPEED S.S.	L_L Peak	L_L S.S.	L_R Peak	L_R S.S.	ΔY_{LF} Peak	ΔY_{LF} S.S.	ΔY_{RR} Peak	ΔY_{RR} S.S.	ΔX_{LF} Peak	ΔX_{LF} S.S.	ΔX_{LR} Peak	ΔX_{LR} S.S.
22 ASC(1R)	3	12	11	900	100	800	250	-.015	-.005	-.011	-.002	-.038	-.031	-.045	-.034
22 ASC(2R)		32	31	-300	-150	1400	400	-.014	-.002	-.013	-.001	-.038	-.030	-.047	-.034
22 ASC(3R)		40	36	-500	-100	2400	700	-.012	-.001	-.013	-.001	-.044	-.034	-.048	-.030
22 ASC(4R)		45	45	1300	500	3000	1300	.018	.002	-.020	-.003	-.041	-.030	-.064	-.048
22 ASC(5R)															
22 ASC(1R)	311	12	11	-600	-500	1250	250	-.015	-.001	.007	.000	-.041	.036	.032	.027
22 ASC(2R)		27	26	-400	-50	1200	300	-.015	.000	.011	.003	.041	.037	.033	.030
22 ASC(3R)		36	35	900	150	1150	50	-.020	-.002	.022	.005	.038	.034	.034	.028
22 ASC(4R)		42	42	1600	600	800	50	-.018	-.003	.027	.007	.036	.029	.022	.015
22 ASC(5R)															
22 ASC(1R)	37	13	12	900	0.0	500	250	-.016	-.007	-.020	-.006	-.044	-.037	-.054	-.050
22 ASC(2R)		32	28	-500	-200	2400	500	-.009	-.001	-.019	-.004	-.049	-.038	-.057	-.049
22 ASC(3R)		41	36	-250	-200	2200	1000	.018	.003	-.023	-.004	-.048	-.042	-.073	-.058
22 ASC(4R)		42	38	-200	-100	2300	1250	.019	.002	-.022	-.004	-.053	-.045	-.087	-.071
22 ASC(5R)															
22 ASC(1R)	43	21	20	1100	650	1100	150	-.014	-.022	-.016	.000	-.028	-.020	-.034	-.021
22 ASC(2R)		42	42	1400	550	2200	250	-.021	-.001	-.017	.000	-.027	-.019	-.041	-.019
22 ASC(3R)		53	52	1600	500	3300	1400	.021	.002	-.018	-.001	-.029	-.019	-.041	-.018
22 ASC(4R)		57	54	900	250	2950	750	.021	.003	-.023	-.004	-.023	-.014	-.064	-.038
22 ASC(5R)															
22 ASC(1R)	49	13	12	1200	200	1900	500	.018	.001	.015	.003	-.031	-.027	-.034	-.026
22 ASC(2R)		25	24.5	-400	-100	800	100	.015	.000	.015	.004	-.034	-.028	-.045	-.029
22 ASC(3R)		38	37.5	-250	-200	1350	500	.021	.003	.017	.001	-.037	-.029	-.039	-.027
22 ASC(4R)		40	38.5	1300	500	3600	1200	.020	.002	.017	.001	-.037	-.030	-.056	-.038
22 ASC(5R)															
22 ASC(1R)															
22 ASC(2R)	157	48	45	-300	-200	900	010	.014	.001	-.019	-.003	.011	.002	-.013	-.003
22 ASC(3R)															
22 ASC(4R)															
22 ASC(5R)															

SERIES A - ROUTE EVALUATION, FORWARD - INSTRUMENTED AXLE IN LEAD

	Curve Number	SPEED	L_L		L_R		ΔY_{LF}		ΔY_{RR}		ΔX_{LF}		ΔX_{LR}	
			Peak	S.S.	Peak	S.S.	Peak	S.S.	Peak	S.S.	Peak	S.S.	Peak	S.S.
22 ARE (F)	3	44	2000	700	8500	4000			-.012	-.006	-.052	-.040	-.044	-.032
22 ARE (EB)		46	2500	1200	9400	4500			+.016	-.008	-.048	-.032	-.044	-.032
22 ARE (F)	311	42	11250	6000	3500	3000			+.024	+.012	+.032	+.020	.040	.036
22 ARE (EB)		42	11500	6000	3500	3000			+.012	+.005	+.032	+.024	+.032	+.038
22 ARE (F)	37	37	3000	2500	9500	6000			-.018	-.008	-.052	-.040	-.060	-.052
22 ARE (EB)		38	3000	2500	9500	6000			-.024	-.008	-.052	-.040	-.064	-.056
22 ARE (F)	43	60	2500	1000	6500	3500			+.020	-.008	-.044	-.024	-.030	-.020
22 ARE (EB)		62	2500	1000	7000	35000			-.024	-.008	-.048	-.032	-.040	-.028
22 ARE (F)	49	42	2500	2000	8500	4500			+.028	+.012	+.048	+.032	+.048	+.040
22 ARE (EB)		38	3000	2000	9000	5000	-.020	-.008	+.028	+.008	+.040	+.032	+.052	+.040
22 ARE (F)	157	50	2500	1250	5000	2000			-.020	-.008	+.032	+.016	+.028	-.016
22 ARE (EB)		50	2000	1000	5000	2000	-.028	-.004	-.024	-.008	-.032	-.012	-.024	-.012

SERIES A - ACCELERATION IN CURVES

Run Number	Curve Number	SPEED Max.	SPEED Min.	L_L Peak	L_L S.S.	L_R Peak	L_R S.S.	ΔY_{LF} Peak	ΔY_{LF} S.S.	ΔY_{RR} Peak	ΔY_{RR} S.S.	ΔX_{LF} Peak	ΔX_{LF} S.S.	ΔX_{RF} Peak	ΔX_{RF} S.S.
23 ATR3P3	3	32	21	3000	1450	6750	3000	.008	-.001	-.016	-.008	-.030	-.020	-.034	-.028
23 ATR3P4	3	43	14	3150	1450	8300	3200	.012	.001	-.017	-.005	-.043	-.019	-.059	-.046
23 ATR37P3	37	28	8	4100	2850	8350	5000	.017	.003	-.015	-.010	-.054	-.041	-.045	-.036
23 ATR37P4	37	41	16	3800	2500	9400	5600	.018	.008	-.019	-.011	-.062	-.042	-.070	-.051
23 ATR157P3	157	40	10	2500	1400	3800	1300	.027	.008	.020	.009	-.034	-.009	-.017	-.008
23 ATR157P4	157	48	16	2450	1100	4200	1300	.028	.008	.021	.008	-.031	-.010	-.023	-.015

SERIES A - STABILITY RUNS

Run Number	Speed (mph)		Peak Measurements - Absolute and Level Exceeded for 100 ms													
			L_L (kips)		L_R (kips)		a_yA-1 (g's)		a_yA-2 (g's)		a_yA-3 (g's)		$\Delta_y LF$ (in)		$\Delta_y RR$ (in)	
	min	max	abs	100ms	abs	100ms	abs	100ms	abs	100ms	abs	100ms	abs	100ms	abs	100ms
22AST35	30	36	3.5	3.5	2.5	1.5	.16	.08	.12	.04	.21	.08	.020	.012	.014	.012
22AST55	aborted															
22AST75	60	78	4.2	2.5	2.6	1.5	.38	.04	.22	.06	.41	.08	.018	.010	.016	.010
Reverse Runns																
22AST35R	32	36	.5	.5	.2	.2	-	-	.30	.04	.18	.04	.020	.014	.018	.012
22AST55R	56	56	1.0	.5	1.0	.2	.43	.05	.54	.06	.41	.05	.018	.010	.016	.012
22AST55R	62	74	1.0	.4	1.5	.2	.50	.06	.54	.09	.40	.10	.020	.012	.014	.010

SERIES B - STEADY CURVING, FORWARD

	Curve Number	SPEED Min.	SPEED Max.	L_L Peak	L_L S.S.	L_R Peak	L_R S.S.	ΔY_{LF} Peak	ΔY_{LF} S.S.	ΔY_{RR} Peak	ΔY_{RR} S.S.	ΔX_{LF} Peak	ΔX_{LF} S.S.	ΔX_{RF} Peak	ΔX_{RF} S.S.
10 BSC(1)	3	9	10	3300	2300	4500	1500	+.004	+.001	+.016	+.008	-.012	-.004	+.020	+.008
10 BSC(2)		19	30	3800	1800	4750	1000	+.022	+.012	+.016	+.008	-.054	-.040	+.058	+.044
10 BSC(3)		24	40	3050	1800	5250	1250	+.024	+.012	+.020	+.012	-.056	-.044	+.056	+.044
10 BSC(4)		34	44	2550	1200	6250	1500	+.028	+.020	+.016	+.008	-.056	-.040	+.054	+.040
10 BSC(5)															
10 BSC(1)	311	8	12	6000	3500	5800	3300	+.020	+.012	+.012	+.008	+.020	+.012	-.020	-.012
10 BSC(2)		24	26	7750	4000	5300	3800			+.010	+.004	+.036	+.028	-.028	-.020
10 BSC(3)		33	36	8250	4500	4800	3300			+.012	+.004	+.036	+.028	-.032	-.020
10 BSC(4)		39	42	9500	4500	3800	2800			+.012	+.004	+.036	+.024	-.036	-.024
10 BSC(5)															
10 BSC(1)	37	8	12	5300	4300	6500	3500			+.012	+.006	-.036	-.032	+.068	-.064
10 BSC(2)		24	26	4800	3800	7500	4000			+.012	+.004	-.052	-.040	+.060	+.052
10 BSC(3)		32	36	4300	3300	8000	4000	+.032	+.020	+.012	-.008	-.060	-.048	+.060	+.052
10 BSC(4)		36	40	3550	2300	8000	3500	+.028	+.020	+.016	+.008	-.060	-.048	-.060	+.052
10 BSC(5)															
10 BSC(1)	43	20	20	3300	1800	2500	500	+.016	+.008	+.012	+.004	-.040	-.028	+.056	+.040
10 BSC(2)		40	40	3050	1300	3000	700	+.024	+.012	+.020	+.008	-.048	-.028	+.056	+.040
10 BSC(3)		48	41	2550	1300	3250	500	+.024	+.008	+.020	+.008	-.052	-.032	+.052	+.032
10 BSC(4)		49	40	4800	130	3250	500	+.010	+.008	+.020	+.012	-.056	-.036	+.040	+.024
10 BSC(5)															
12 BSC(1)	49	8	12	5300	3800	5000	3000			+.010	+.008	-.025	-.016	+.048	+.054
12 BSC(2)		17	18	4300	3300	6000	2500	+.020	+.016	+.016	+.012	-.048	-.036	+.032	+.028
12 BSC(3)		36	37	3050	2300	2000	3000	+.024	+.016	+.012	+.006	-.052	-.040	+.046	+.040
12 BSC(4)		40	42	2800	2050	7500	3000			+.010	+.006	-.052	-.040	+.046	+.036
12 BSC(5)															
12 BSC(1)	157	20	20	3050	1800	1500	0			+.012	+.008	-.036	-.024	+.048	+.030
12 BSC(2)		44	50	2800	1550	2250	250	+.020	+.012	-.016	+.008	-.034	-.020	+.052	+.032
12 BSC(3)		52	56	2300	1000	2250	700	+.020	+.012	+.012	+.004	-.040	-.024	+.048	+.032
12 BSC(4)		50	52	2550	1300	2750	700			+.008	+.004	-.048	-.024	+.048	+.028
12 BSC(5)															

SERIES B - STEADY CURVING, REVERSE

	Curve Number	SPEED		L_L		L_R		ΔY_{LF}		ΔY_{RR}		ΔX_{LF}		ΔX_{RF}	
		Min.	Max.	Peak	S.S.	Peak	S.S.	Peak	S.S.	Peak	S.S.	Peak	S.S.	Peak	S.S.
10 BSC(1R)	3	10	12	1000	0	550	250			-.024	-.018	-.026	-.022	+.032	+.020
10 BSC(2R)		29	32	250	0	1000	550	-.020	-.012	-.024	-.020	-.030	-.024	+.039	+.020
10 BSC(3R)		39	40	0	0	1500	800	-.020	-.012	-.026	-.020	-.028	-.020	+.028	+.016
10 BSC(4R)		46	47	0	0	2250	1000	-.016	-.006	-.028	-.020	-.028	-.018	+.024	+.014
10 BSC(5R)															
10 BSC(1R)	311	10	11	700	250	1550	500			+.018	+.010	+.028	+.024	-.024	-.018
10 BSC(2R)		22	28	1000	0	800	0			+.024	+.014	+.026	+.012	-.024	-.016
10 BSC(3R)															
10 BSC(4R)															
10 BSC(5R)															
10 BSC(1R)	37	10	12	800	250	800	500	-.022	-.012	-.028	-.018	-.028	-.024	+.044	+.038
10 BSC(2R)		35	37	250	0	1500	800	-.014	-.012	-.022	-.020	-.030	-.026	+.040	+.032
10 BSC(3R)		33	38	250	0	2250	1000	-.022	-.010	-.032	-.020	-.034	-.026	+.036	+.028
10 BSC(4R)		37	41	250	0	2500	1500	-.024	-.008	-.032	-.020	-.034	-.024	+.036	+.028
10 BSC(5R)															
10 BSC(1R)	43	20	21	750	0	550	250	-.018	-.014	-.022	-.016	-.016	-.012	+.024	+.016
10 BSC(2R)		41	43	250	0	1000	550	-.022	-.014	-.024	-.016	-.024	-.016	+.018	+.010
10 BSC(3R)		48	53	0	0	1750	800	-.024	-.012	-.020	-.016	-.026	-.020	+.024	+.012
10 BSC(4R)		48	54	250	0	1500	800	-.020	-.010	-.020	-.016	-.026	-.020	+.010	+.008
10 BSC(5R)															
12 BSC(1R)	49	9	11		500	800	250			-.024	-.016	-.034	-.030	+.040	+.028
12 BSC(2R)		25	26	1050	250	1050	500			-.018	-.012	-.040	-.032	+.040	+.028
12 BSC(3R)		36	36	250	0	1750	800			-.020	-.016	-.034	-.024	+.028	+.020
12 BSC(4R)		40	41	0	0	2250	1000			-.020	-.020	-.028	-.016	+.032	+.024
12 BSC(5R)															
12 BSC(1R)	157	19	22	3250	1000	550	0			-.016	-.008	-.028	-.016	+.030	+.016
12 BSC(2R)		45	46	2000	550	1050	500	+.012	+.002	-.016	-.008	-.028	-.016	+.026	+.012
12 BSC(3R)		54	57	1750	500	1500	750			-.012	-.008	-.028	-.018	+.026	+.012
12 BSC(4R)		54	58	1250	500	1250	750			-.016	-.010	-.030	-.020	+.028	+.008
12 BSC(5R)															

SERIES B - ROUTE EVALUATION, FORWARD

	Curve Number	SPEED		L_L		L_R		Y_{LF}		ΔY_{RR}		ΔX_{LF}		ΔX_{RF}	
		Min.	Max.	Peak	S.S.	Peak	S.S.	Peak	S.S.	Peak	S.S.	Peak	S.S.	Peak	S.S.
10 BRE (F)	3	42	46	1800	800	6500	1500	.028	.018	.016	.007	-.068	-.056	.052	.044
10 BRE (FB)		6	34	4300	2800	6750	2000	+.028	+.010	+.012	+.004	-.040	-.028	+.060	+.052
12 BRE (F)		46	48	2050	800	7500	3000			+.028	+.012	-.076	-.064	+.052	+.040
12 BRE (FB)		44	47	2300	1050	7250	2000			+.014	+.006	+.046	-.032	+.048	+.040
10 BRE (F)	311	42	45	8750	4000	2800	1800	.016	-.006	.016	.008	.044	.036	-.040	-.036
10 BRE (FB)		42	44	9500	5600	3050	1800			+.012	+.004	+.032	+.024	-.052	-.044
12 BRE (F)		43	44	9750	4500	3300	2300			+.018	+.008	+.032	+.024	-.052	-.044
12 BRE (FB)		40	44	9500	4500	3300	2050			+.012	+.004	+.036	+.028	-.032	-.020
10 BRE (F)	37	37	40	3300	2300	7250	3500	+.040	+.012	+.016	+.004	-.064	-.048	+.068	+.060
10 BRE (FB)		36	37	3550	3400	9750	5000	+.032	+.024	+.016	+.006	-.056	-.044	+.056	+.048
12 BRE (F)		36	40	3800	3300	7250	4000			+.008	+.004	-.076	-.064	+.072	+.060
12 BRE (FB)		37	40	3550	2800	7250	5000			+.010	+.004	-.052	-.040	+.060	+.048
10 BRE (F)	43	48	54	1800	800	3750	1000	+.028	+.020	+.020	+.012	-.068	-.042	+.040	+.020
10 BRE (FB)		45	54	1800	800	3500	800	+.018	+.012	+.010	+.010	-.052	-.035	+.040	+.028
12 BRE (F)		60	63	1550	550	4500	1500			+.020	+.008	-.056	-.036	+.056	+.040
12 BRE (FB)		60	62	1800	800	4500	1000			+.016	+.008	-.046	-.028	+.048	+.032
10 BRE (F)	49														
10 BRE (FB)															
12 BRE (F)		43	44	2800	1800	7250	4000			+.012	+.004	-.048	-.040	+.064	+.056
12 BRE (FB)		43	44	3300	1800	8000	3000			+.010	+.006	-.056	-.044	+.052	+.044
10 BRE (F)	157														
10 BRE (FB)															
12 BRE (F)		55	64	2300	800	2250	800			+.012	+.006	-.040	-.028	+.050	+.028
12 BRE (FB)		54	62	2300	1300	2500	800			+.012	+.006	-.042	-.024	+.052	+.032

SERIES B - ROUTE EVALUATION, REVERSE

	Curve Number	SPEED		L_L		L_R		ΔY_{LF}		ΔY_{RR}		ΔX_{LF}		ΔX_{RF}	
		Min.	Max.	Peak	S.S.	Peak	S.S.	Peak	S.S.	Peak	S.S.	Peak	S.S.	Peak	S.S.
10 BRE (R)	3	48	49	0	0	2800	1250	-.020	-.010	-.032	-.024	-.038	-.026	+.024	+.016
12 BRE (R)		48	49	250	0	2750	1800			-.024	-.016	-.022	-.012	+.028	+.014
10 BRE (R)	311	36	44	1800	800	500	0	-.010	-.006	+.034	+.020	+.030	+.022	-.024	-.020
12 BRE (R)		11	14	750	250	2000	750			+.014	+.008	+.038	+.030	-.012	-.010
10 BRE (R)	37	38	39	0	0	2500	1500	-.016	-.012	-.028	-.024	-.044	-.036	+.034	+.028
12 BRE (R)		37	40	250	0	2500	1500			-.022	-.018	-.026	-.018	+.020	+.012
10 BRE (R)	43	52	56	0	0	1500	800	-.020	-.014	-.036	-.020	-.016	-.012	+.028	+.020
12 BRE (R)		56	61	250	0	2000	1000			-.024	-.018	-.014	-.004	+.028	+.020
12 BRE (R)	49	42	44	500	0	2750	1500			-.028	-.020	-.018	-.014	+.030	+.020
12 BRE (R)	157	56	62	1250	500	1750	800			-.018	-.012	-.024	-.012	+.016	+.012

SERIES B - ACCELERATION IN CURVES

Run Number	Curve Number	SPEED		L_L		L_R		ΔY_{LF}		ΔY_{RR}		ΔX_{LF}		ΔX_{RF}	
		Max.	Min.	Peak	S.S.	Peak	S.S.	Peak	S.S.	Peak	S.S.	Peak	S.S.	Peak	S.S.
10-BTR3P3	3	34	-	4300	2800	6000	1500	+.012	+.008	+.012	+.008	-.040	-.028	+.060	+.052
10-BTR3P4	3	44	-	4300	2800	6000	2000	+.028	+.020	+.016	+.008	-.040	-.028	+.060	+.052
10-BTR37P3	37	32	-	5800	4300	7000	4500	+.028	+.016	+.012	+.004	-.048	-.036	+.060	+.052
10-BTR37P4	37	42	-	5550	4050	8000	4500	+.028	+.020	+.012	+.004	-.060	-.032	+.000	+.052
12-BTR157P3	157	44	-	3300	1800	2000	500			+.004	+.002	-.032	-.020	+.048	+.032
12-BTR157P4	157	54	-	3300	1800	2500	800			+.012	+.004	-.032	-.016	+.048	+.032

SERIES B - STABILITY RUNS

Run	Speed (mph)		Peak Measurements - Absolute and Level Exceeded for 100 ms											
			L_L (kips)		L_R (kips)		a_yA-1 (g's)		a_yA-2 (g's)		a_yA-3 (g's)		$\Delta_y LF$ (in)		$\Delta_y RR$ (in)	
Number	min	max	abs	100ms	abs	100ms	abs	100ms	abs	100ms	abs	100ms	abs	100ms	abs	100ms
12BST(35)	35	37	2250	2000	2000	1250	.14	.04	.14	.04	.20	.08	.004	.004	.008	.006
12BST(55)	55	57	2250	1000	2250	1000	.24	.12	.26	.08	.28	.08	.006	.004	.012	.008
12BST(75)	56	69	2750	1250	2000	1000	.28	.10	.32	.08	.028	.08	.010	.010	.012	.008
Reverse Runs																
12BST(35R)	35	36	1200	1250	1750	750	.12	.04	.12	.06	.12	.04	.010	.010	.006	.006
12BST(55R)	56	58	1250	1000	1750	750	.30	.08	.30	.08	.20	.04	.008	.004	.010	.004
12BST(75R)	72	77	1500	1000	1700	500	.32	.10	.44	.08	.34	.06	.010	.012	.014	.008

SERIES C - STEADY CURVING, FORWARD

	Curve Number	SPEED		L_L		L_R		ΔY_{LF}		ΔY_{RR}		ΔX_{LF}		ΔX_{RF}	
		Min.	Max.	Peak	S.S.	Peak	S.S.	Peak	S.S.	Peak	S.S.	Peak	S.S.	Peak	S.S.
19 CSC(1)	3	10	15	2500	2000	4000	1500	+.024	+.016	+.012	+.010	-.032	-.028	+.036	+.028
19 CSC(2)		25	26	2000	1500	4250	1250	+.020	+.012	+.012	+.008	-.032	-.024	+.036	+.032
19 CSC(3)		42	44	1750	1000	6250	2000	+.016	+.008	+.008	+.004	-.042	-.032	-.020	+.018
19 CSC(4)		46	48	1500	1000	6500	2500	+.016	+.008	+.012	+.006	-.040	-.032	+.028	+.020
19 CSC(1)	311	8	10	5000	2500	3750	2500	-.014	-.004	-.016	-.004	+.028	+.024	-.016	-.012
19 CSC(2)		22	25	6000	3500	3500	2000	-.016	-.008	-.010	-.008	+.028	+.020	-.016	-.004
19 CSC(3)		33	37	6750	4000	3000	2250	-.022	-.010	-.018	-.008	+.020	+.014	-.024	-.020
19 CSC(4)		40	41	7500	4000	2500	1750	-.024	-.012	-.014	-.006	+.016	+.008	-.028	-.024
19 CSC(1)	37	8	12	3500	2500	4750	2500	+.020	+.012	+.010	+.008	-.032	-.028	+.032	+.028
19 CSC(2)		24	27	3500	2250	6000	3250	+.028	+.016	+.008	+.006	-.036	-.028	+.048	+.042
19 CSC(3)		33	36	3500	2500	7000	3500	+.024	+.012	+.004	+.002	-.040	-.032	+.044	+.040
19 CSC(4)		38	41	3000	2000	7250	3500	+.024	+.012	+.004	+.002	-.048	-.040	+.040	+.032
19 CSC(1)	43	19	20	2500	1500	2250	500	+.016	+.008	+.014	+.010	-.032	-.024	+.036	+.028
19 CSC(2)		42	42	2500	1750	2750	1000	+.020	+.012	+.014	+.010	-.032	-.020	+.036	+.030
19 CSC(3)		50	51	2500	1500	3000	1000	+.018	+.008	+.010	+.008	-.036	-.024	+.034	+.026
19 CSC(4)		63	65	2000	750	4500	1500	+.016	+.008	+.016	+.010	-.042	-.032	+.026	+.020
19 CSC(1)	49	9	10	3250	2000	3500	2000	+.020	+.012	+.012	+.010	-.028	-.020	+.032	+.028
19 CSC(2)		25	27	3250	2250	6000	2500	+.020	+.012	+.012	+.010	-.032	-.024	+.032	+.028
19 CSC(3)		47	49	3000	2500	6750	3000	+.020	+.010	+.008	+.004	-.036	-.028	+.032	+.028
19 CSC(4)		42	42	2750	1500	6750	3000	+.022	+.012	+.012	+.008	-.042	-.036	+.030	+.026
19 CSC(1)	157	18	25	3000	1500	2000	0	+.016	+.004	+.014	+.012	-.020	-.016	+.030	+.022
19 CSC(2)		44	45	2500	1500	2250	500	+.016	+.004	+.012	+.006	-.034	-.024	+.028	+.020
19 CSC(3)		58	59	2500	1000	2500	500	+.014	+.004	+.014	+.006	-.034	-.016	+.034	+.020
19 CSC(4)		65	67	2000	1000	3000	1000	+.024	+.004	+.020	+.008	-.044	-.024	+.030	+.014

SERIES C - STEADY CURVING, REVERSE

	Curve Number	SPEED		L_L		L_R		ΔY_{LF}		ΔY_{RR}		ΔX_{LF}		ΔX_{RF}	
		Min.	Max.	Peak	S.S.	Peak	S.S.	Peak	S.S.	Peak	S.S.	Peak	S.S.	Peak	S.S.
19 CSC(1R)	3	8	14	1250	0	500	0	-.024	-.008	-.008	-.008	-.016	-.016	.016	.014
19 CSC(2R)		28	28	500	0	750	250	-.020	-.008	-.016	-.016	-.016	-.012	.012	.012
19 CSC(3R)		39	41	500	0	1500	500	-.022	-.008	-.018	-.016	-.020	-.012	.016	.012
19 CSC(4R)		41	45	500	0	1500	1000	-.020	-.008	-.018	-.016	-.016	-.012	.016	.014
19 CSC(1R)	311	8	18	500	0	1500	500	.016	.008	-.010	.002	.020	.018	-.016	-.014
19 CSC(2R)		20	28	500	0	500	0	.028	.012	.012	.008	.022	.020	-.020	-.016
19 CSC(3R)		33	34	750	250	1000	250	.020	.004	.016	.010	.018	.014	-.018	-.016
19 CSC(4R)		32	39	1000	250	1000	500	-.016	.002	.020	.012	.024	.018	.012	.010
19 CSC(1R)	37	8	14	1250	500	500	0	-.032	-.012	-.012	-.012	-.020	-.016	.024	.024
19 CSC(2R)		24	28	750	0	1000	250	-.028	-.012	-.014	-.012	-.028	-.024	.024	.020
19 CSC(3R)		32	37	500	0	1500	500	-.032	-.008	-.016	-.016	-.024	-.022	.022	.018
19 CSC(4R)		38	42	250	0	2000	1000	-.024	-.012	-.024	-.020	-.034	-.020	.016	.016
19 CSC(1R)	43	20	20	500	0	500	0	.026	.016	-.016	-.016	-.016	-.014	.008	.008
19 CSC(2R)		40	40	500	0	1250	500	-.022	-.012	-.020	-.018	-.014	-.004	.008	.006
19 CSC(3R)		49	50	250	0	1500	500	-.024	-.010	-.018	-.016	-.016	-.010	.012	.008
19 CSC(4R)		58	58	0	0	2000	1000	-.022	-.006	-.020	-.016	-.014	-.004	.012	.008
19 CSC(1R)	49	8	12	2000	500	500	0	-.028	-.016	-.016	-.014	-.020	-.016	.016	.014
19 CSC(2R)		24	26	1000	0	1000	0	-.024	-.012	-.020	-.014	-.028	-.026	.020	.016
19 CSC(3R)		33	35	500	0	1500	500	-.026	-.012	-.022	-.014	-.032	-.022	.020	.016
19 CSC(4R)		34	40	500	0	2000	750	-.032	-.012	-.020	-.016	-.036	-.024	.020	.014
19 CSC(1R)	157	18	20	2000	500	1000	0	-.034	-.012	-.016	-.008	-.012	-.004	.008	.004
19 CSC(2R)		45	46	1000	0	750	0	-.024	-.008	-.016	-.012	-.016	-.008	.012	.006
19 CSC(3R)		54	56	500	0	1000	250	-.028	-.008	-.020	-.006	-.016	-.008	.016	.012
19 CSC(4R)		60	65	500	0	1500	500	-.020	-.008	-.016	-.008	-.014	-.008	.012	.008

SERIES C - ROUTE EVALUATION, FORWARD

	Curve	SPEED		L_L		L_R		ΔY_{LF}		ΔY_{RR}		ΔX_{LF}		ΔX_{RF}	
	Number	Min.	Max.	Peak	S.S.	Peak	S.S.	Peak	S.S.	Peak	S.S.	Peak	S.S.	Peak	S.S.
19 CRE(F)	3	38	43	2500	1500	5250	2000	+.020	+.012	+.004	.002	-.040	-.030	+.032	+.020
19 CRE(F)	311	32	32	6500	4000	3250	2000	-.022	-.008	-.022	-.008	+.022	+.020	-.020	-.018
19 CRE(F)	37	32	33	3250	2500	6500	3000	+.024	+.012	+.004	+.002	-.040	-.036	+.040	+.032
19 CRE(F)	43	41	43	3000	2000	3500	750	+.018	+.008	+.014	+.008	-.040	-.024	+.036	+.030
19 CRE(F)	49	41	42	2750	2000	6750	3000	+.024	+.014	+.008	+.004	-.044	-.036	+.028	+.024
19 CRE(F)	157	52	54	2500	1500	2000	500	+.010	+.004	+.010	+.004	-.042	-.028	+.024	+.012

SERIES C - ROUTE EVALUATION, REVERSE

	Curve Number	SPEED		L_L		L_R		ΔY_{LF}		ΔY_{RR}		ΔX_{LF}		ΔX_{RF}	
		Min.	Max.	Peak	S.S.	Peak	S.S.	Peak	S.S.	Peak	S.S.	Peak	S.S.	Peak	S.S.
19 CRE(R)	3	31	32	500	0	1000	0	-.024	-.012	-.016	-.14	-.020	-.016	.016	.012
19 CRE(R)	311	0	25	500	0	1500	250	.028	.012	.020	.012	.024	.022	-.016	-.012
19 CRE(R)	37	36	38	500	0	1750	750	-.020	-.008	-.018	-.016	-.026	-.018	.028	.024
19 CRE(R)	43	50	50	500	0	1250	500	-.024	-.012	-.018	-.016	-.020	-.012	.018	.014
19 CRE(R)	49	42	44	500	0	2500	1000	-.036	-.008	-.028	-.016	-.040	-.032	.030	.024
19 CRE(R)	157	53	58	500	0	1000	250	-.034	-.008	-.026	-.008	-.018	-.008	.012	.006

SERIES C - (BALLASTED) STEADY CURVING, FORWARD

	Curve Number	SPEED		L_L		L_R		ΔY_{LF}		ΔY_{RR}		ΔX_{LF}		ΔX_{RF}	
		Min.	Max.	Peak	S.S.	Peak	S.S.	Peak	S.S.	Peak	S.S.	Peak	S.S.	Peak	S.S.
20 CSC(1)	3	19	20	2750	1750	4000	1000	+.026	+.012	+.018	+.014	-.036	-.028	+.046	+.042
20 CSC(2)		29	30	2250	1250	4500	1500	+.022	+.012	+.018	+.012	-.040	-.030	+.038	+.032
20 CSC(3)		40	41	1750	1000	6000	1750	+.024	+.016	+.014	+.008	-.040	-.028	+.030	+.028
20 CSC(4)		43	46	1500	1000	6500	2000			+.010	+.006	-.044	-.036	+.016	+.012
20 CSC(5)		48	50	1250	750	8250	2500			+.016	+.008	-.044	-.036	+.024	+.020
20 CSC(1)	311	12	14	6500	4000	4500	3000	-.016	-.002	-.016	-.008	+.036	+.030	-.022	-.018
20 CSC(2)		22	24	6500	4000	4000	3000	-.008	-.002	-.014	-.008	+.030	+.024	-.024	-.022
20 CSC(3)		32	35	8000	4000	3500	2000	-.018	-.006	-.012	-.004	+.028	+.020	-.024	-.020
20 CSC(4)		38	39	9000	5000	3500	2000			+.014	+.004	+.024	+.014	-.022	-.016
20 CSC(5)		42	44	9200	5500	3250	2000			+.012	+.004	+.024	+.010	-.030	-.024
20 CSC(1)	37	10	14	5000	3500	6000	3000	+.026	+.014	+.014	+.012	-.028	-.024	+.028	+.026
20 CSC(2)		22	25	5000	3500	6250	3250	+.028	+.018	+.010	+.008	-.046	-.044	+.050	+.048
20 CSC(3)		32	35	3500	2500	7750	3000	+.036	+.020	+.012	+.006	-.052	-.042	+.056	+.044
20 CSC(4)		36	40	3600	2400	8000	3400			+.010	+.004	-.052	-.044	+.056	+.046
20 CSC(5)		39	44	3250	2250	7700	3500			+.016	+.006	-.050	-.046	+.048	+.044
20 CSC(1)	43	18	20	3600	2000	2500	250	+.022	+.012	+.016	+.016	-.032	-.026	+.048	+.042
20 CSC(2)		35	38	3250	2000	3250	250	+.022	+.012	+.020	+.012	-.040	-.028	+.040	+.034
20 CSC(3)		48	49	2500	1250	3000	750	+.022	+.016	+.014	+.012	-.040	-.028	+.032	+.028
20 CSC(4)		57	58	2000	1000	3750	1000			+.020	+.012	-.040	-.030	+.034	+.028
20 CSC(5)		61	62	1500	500	4250	1000			+.020	+.010	-.044	-.032	+.032	+.024
20 CSC(1)	49	13	15	3500	2250	4250	1750	+.020	+.010	+.016	+.014	-.034	-.028	+.046	+.042
20 CSC(2)		23	25	3500	2250	5000	2000	+.020	+.012	+.014	+.010	-.040	-.032	+.036	+.034
20 CSC(3)		34	35	3000	1750	6000	2500	+.024	+.018	+.012	+.010	-.040	-.032	+.032	+.030
20 CSC(4)		38	42	2600	1500	7100	3000			+.012	+.008	-.040	-.032	+.036	+.032
20 CSC(5)		44	46	2250	1000	8500	3500			+.020	+.008	-.040	-.032	+.032	+.028
20 CSC(1)	157	24	25	3250	1500	1500	0	+.018	+.004	+.016	+.012	-.026	-.022	+.044	+.032
20 CSC(2)		42	46	2500	1250	2000	250	+.018	+.004	+.016	+.010	-.036	-.022	+.036	+.024
20 CSC(3)		64	66	2500	1250	2000	250	+.018	+.004	+.020	+.012	-.038	-.024	+.036	+.022
20 CSC(4)		62	66	2000	1000	2750	500			+.016	+.008	-.040	-.024	+.044	+.028
20 CSC(5)		60	66	2000	750	2500	500			+.020	+.008	-.040	-.020	+.040	+.020

SERIES C - (BALLASTED) STEADY CURVING, REVERSE

	Curve Number	SPEED Min.	SPEED Max.	L_L Peak	L_L S.S.	L_R Peak	L_R S.S.	ΔY_{LF} Peak	ΔY_{LF} S.S.	ΔY_{RR} Peak	ΔY_{RR} S.S.	ΔX_{LF} Peak	ΔX_{LF} S.S.	ΔX_{RF} Peak	ΔX_{RF} S.S.
20 CSC(1R)	3	19	20	1250	250	750	250	-.028	-.016	-.012	-.012	-.018	-.010	.018	.016
20 CSC(2R)		28	30	500	0	750	250	-.020	-.016	-.016	-.012	-.016	.008	.016	.014
20 CSC(3R)		38	40	500	0	1750	750	-.022	-.012	-.020	-.018	-.020	-.008	.012	.010
20 CSC(4R)		42	46	500	0	2250	1000			-.024	-.020	-.016	-.008	.016	.012
20 CSC(5R)		48	50	500	0	2500	1500			-.024	-.020	-.018	-.012	-.008	-.006
20 CSC(1R)	311	14	14	1000	250	1500	250	.028	.008	.015	.008	.028	.024	-.008	-.006
20 CSC(2R)		24	24	1500	500	1000	0	.020	.008	.016	.010	.028	.024	-.010	-.008
20 CSC(3R)		33	35	1500	750	1000	0	.028	.004	.022	.016	.020	.016	-.022	-.020
20 CSC(4R)		40	40	2000	1000	500	0			.026	.016	.022	.016	-.018	-.012
20 CSC(5R)		44	45	2500	1500	500	0			.028	.020	.018	.012	-.020	-.016
20 CSC(1R)	37	15	16	1500	500	1250	250	.040	.024	-.014	-.012	-.020	-.012	.024	.020
20 CSC(2R)		22	27	1000	0	1200	250	-.038	-.016	-.020	-.018	-.020	-.012	.030	.028
20 CSC(3R)		32	38	500	0	2000	1000	-.040	-.012	-.028	-.020	-.024	-.012	.022	.020
20 CSC(4R)		32	42	250	0	2500	1500			-.034	-.020	-.028	-.020	.024	.020
20 CSC(5R)		34	46	500	0	3500	2000			-.032	-.016	-.028	-.020	.024	.020
20 CSC(1R)	43	20	20	1500	250	250	0	-.028	-.012	-.020	-.014	-.020	-.016	.012	.008
20 CSC(2R)		40	40	500	0	1500	500	-.026	-.016	-.016	-.012	-.014	-.010	.010	.009
20 CSC(3R)		50	50	500	0	1500	500	-.034	-.016	-.024	-.016	-.012	-.004	.010	.008
20 CSC(4R)		60	60	250	0	2000	1500			-.020	-.014	-.014	-.006	-.008	-.002
20 CSC(5R)		62	64	250	0	3000	1500			-.022	-.016	-.016	-.008	.014	.010
20 CSC(1R)	49	15	15	2000	750	750	0	-.016	-.008	.004	.002	-.015	-.009	.016	.012
20 CSC(2R)		23	25	1250	0	1000	250	-.030	-.016	-.018	-.008	-.020	-.014	.028	.012
20 CSC(3R)		30	34	500	0	1500	500	-.038	-.020	-.016	-.012	-.020	-.012	.020	.012
20 CSC(4R)		38	40	500	0	2000	1000			-.014	-.008	-.020	-.008	.022	.016
20 CSC(5R)		43	44	500	0	3000	1500			-.028	-.020	-.026	-.012	.020	.012
20 CSC(1R)	157	24	25	2750	750	0	0	-.028	-.016	-.004	-.004	-.018	-.014	.020	.012
20 CSC(2R)		44	46	1750	250	500	0	-.028	-.012	-.010	-.004	-.020	-.012	.010	.004
20 CSC(3R)		49	55	1000	250	1000	250	-.038	-.016	-.020	-.004	-.020	-.010	.016	.008
20 CSC(4R)		55	60	1000	250	1250	500			-.016	-.012	-.020	-.012	.016	.008
20 CSC(5R)		60	62	1000	250	1500	500			-.018	-.008	-.012	-.004	.016	.008

SERIES C - STABILITY RUNS

Run Number	Speed (mph)		Peak Measurements - Absolute and Level Exceeded for 100 ms													
			L_L (kips)		L_R (kips)		$a_y A$-1 (g's)		$a_y A$-2 (g's)		$a_y A$-3 (g's)		$\Delta_y LF$ (in)		$\Delta_y RR$ (in)	
	min	max	abs	100ms	abs	100ms	abs	100ms	abs	100ms	abs	100ms	abs	100ms	abs	100ms
19C ST35	34	36	2.2	1.5	1.5	1.2	.12	.03	.12	.04	.20	.05	.016	.012.	.008	.008
19C ST55	50	56	2.5	1.5	1.6	1.0	.24	.05	.25	.06	.36	.04	.016	.008	.012	.012
19C ST65	62	68	3.4	1.5	1.6	1.0	34	.05	.30	.07	.44	.06	.016	.008	.012	.012
(rain)																
19C ST75	54	73	3.0	1.0	1.7	1.0	.32	.04	.28	.06	.38	.08	.014	.006	.016	.012
Reverse Runs																
19C ST35R	35	38	.5	.5	.5	.3	.16	.04	.30	.06	.13	.03	.06	.008	.008	.008
19C ST55R	51	56	1.0	.5	1.0	.3	.30	.04	54	.06	.20	.04	.016	.008	.012	.010
19C ST65R	57	67	1.0	.5	1.0	.3	.32	.06	.43	.08	.22	.04	.015	.006	.010	.010
19C ST75R	56	72	1.0	.5	1.0	.3	.32	.06	.42	.07	.22	.06	.016	.006	.020	.020

SERIES C (BALLASTED) - STABILITY RUNS

			Peak Measurements - Absolute and Level Exceeded for 100 ms													
Run Number	Speed (mph)		L_L (kips)		L_R (kips)		a_yA-1 (g's)		a_yA-2 (g's)		a_yA-3 (g's)		Δ_y^{LF} (in)		Δ_y^{RR} (in)	
	min	max	abs	100ms	abs	100ms	abs	100ms	abs	100ms	abs	100ms	abs	100ms	abs	100ms
20C ST35	35	36	2.5	1.5	1.5	1.0	.14	.02	.12	.02	.18	.03	.014	.008	-	-
20C ST55	44	57	3.0	1.2	2.0	1.0	.21	.03	.18	.03	.35	.04	.014	.006		
20C ST65	64	68	2.7	1.0	2.0	1.0	.20	.05	.20	.04	.32	.05	.014	.006		
20C ST75	64	76	3.0	1.0	2.0	1.0	.34	.05	.20	.04	.40	.06	.014	.006		
Reverse Runs																
20C ST35R	37	38	.75	.5	.75	.5	.12	.04	.28	.04	.12	.02	.014	.004	.010	.004
20C ST55R	54	56	1.0	.5	1.0	.5	.32	.04	.44	.04	.26	.04	.014	.012	.012	.004
20C ST55R	58	66	1.5	.5	1.0	.2	.38	.06	.44	.04	.32	.06	.014	.006	.014	.004
20C ST75R	53	74	2.0	.5	1.0	.5	.34	.08	.44	.06	.34	.08	.014	.008	.012	.006

SERIES F - STEADY CURVING

	Curve Number	SPEED		L_L		L_R		ΔY_{LF}		ΔY_{RR}		ΔX_{LF}		ΔX_{RF}	
		Min.	Max.	Peak	S.S.	Peak	S.S.	Peak	S.S.	Peak	S.S.	Peak	S.S.	Peak	S.S.
	3														
	311														
17 FSC(1)	37	14	18	3000	1700	4200	1000	+.032	+.018	+.024	+.008	-.144	-.112	+.180	+.148
17 FSC(1R)		16	18	1500	500	500	0	-.024	-.010	-.046	-.032	-.104	-.064	+.128	+.096
17 FSC(2)		37	38	2000	600	5500	1500	+.032	+.016	+.032	+.020	-.176	-.120	+.232	+.148
	43														
	49														
	157														

SERIES F - STABILITY RUNS

Run	Speed (mph)		Peak Measurements - Absolute and Level Exceeded for 100 ms													
			L_L (kips)		L_R (kips)		a_yA-1 (g's)		a_yA-2 (g's)		a_yA-3 (g's)		Δ_yLF (in)		Δ_yRR (in)	
Number	min	max	abs	100ms	abs	100ms	abs	100ms	abs	100ms	abs	100ms	abs	100ms	abs	100ms
17F ST35	35	36	1500	500	500	500	.14	.06	.12	.04	.20	.04	.016	.008	.010	.010
17F ST55	34	58	1500	500	500	500	.16	.02	.20	.04	.24	.06	.016	.008	.016	.012
17F ST65	35	68	1500	500	500	500	.30	.04	.20	.08	.26	.08	.020	.008	.014	.012
17F ST75	34	65	1500	500	500	500	.30	.02	.16	.04	.26	.04	.016	.008	.016	.012
Reverse Runs																
17F ST35R	34	36	1200	500	500	500	.12	.02	.22	.06	.10	.02	.018	.008	.016	.012
17F ST55R	32	55	1000	500	1000	200	.22	.04	.32	.04	.16	.04	.020	.012	.030	.020
17F ST65R	32	75	1200	500	500	200	.20	/06	.32	.06	.20	.04	.020	.012	.028	.020
17F ST75R	34	75	1200	500	1000	200	.24	.06	.26	.06	.20	.04	.020	.012	.020	.016

SERIES G - STEADY CURVING, FORWARD

	Curve	SPEED		L_L		L_R		ΔY_{LF}		ΔY_{RR}		ΔX_{LF}		ΔX_{RF}	
25 GSC(1)	3	22	23	2000	500	2500	250	+.020	-.010	+.020	+.004	-1.70	-.110	+.160	+.090
25 GSC(2)		28	30	1500	500	3000	500	+.020	+.008	+.024	+.006	-.176	-.104	+.196	+.104
25 GSC(3)		38	42	1500	500	4500	1000			+.020	+.004	-.176	-.96	+.172	+.960
25 GSC(4)		48	48	1250	250	5600	1500	+.028	+.012	+.024	+.008	-.172	-.088	+.176	+.096
25 GSC(5)		48	51	1250	100	7000	1500			+.032	+.012	-.168	-.088	+.180	+.088
25 GSC(1)	311	10	11	2250	750	1500	500	-.028	-.022	-.008	-.002	+.185	+.140	-.195	-.140
25 GSC(2)		22	25	3100	1000	1250	250	-.032	-.016	+.008	0	+.176	+.128	-.236	-.162
25 GSC(3)		32	34	3600	1250	1000	0			+.008	+.004	+.192	+.144	+.232	-.144
25 GSC(4)		37	42	5250	2000	750	0			-.020	-.008	+.124	+.128	-.204	-.152
25 GSC(5)		42	44	7600	2000	750	0			-.014	-.004	+.180	+.088	-.208	-.136
25 GSC(1)	37	8	14	4000	2000	5000	1250	+.020	+.008	+.020	+.008	-.170	-.110	+.195	+.150
25 GSC(2)		22	24	3000	1250	5500	1500	+.020	+.008	+.020	+.008	-.184	-.128	+.208	+.168
25 GSC(3)		32	38	2500	1000	6250	2000	+.028	+.012	+.028	+.020	+.196	-.128	+.216	+.168
25 GSC(4)		36	40	2500	750	7250	2500			+.030	+.016	-.200	-.120	+.212	+.168
25 GSC(5)		44	47	2000	500	7400	2500	-.024	+.008	+.042	+.024	-.228	-.136	+.212	+.152
25 GSC(1)	43	20	22	2500	1000	2000	0	+.020	+.010	+.012	+.004	-.130	-.700	+.150	+.080
25 GSC(2)		37	38	2100	750	2600	250	+.020	+.008	+.008	0	-.152	-.080	+.184	+.088
25 GSC(3)		48	50	1500	250	3000	250	+.020	+.010	+.016	+.008	-.172	-.080	+.180	+.080
25 GSC(4)		58	59	1000	250	4250	500			+.020	+.004	-.172	-.080	+.192	+.088
25 GSC(5)		58	59	1000	250	4000	500	+.024	+.008	+.020	+.006	-.160	-.072	+.164	+.064
25 GSC(1)	49	16	18	3500	2000	3750	1250	+.016	+.008	-.032	-.004	-.150	-.110	+.160	+.130
25 GSC(2)		23	25	3000	1500	4250	1500			+.032	+.004	-.176	-.120	+.176	+.136
25 GSC(3)		33	36	2750	1000	4500	1500	+.036	+.012	+.040	+.016	-.168	-.128	+.164	+.128
25 GSC(4)		38	41	2250	750	5000	2000			+.026	+.008	-.176	-.128	+.192	+.144
25 GSC(5)		44	46	2000	500	5250	2000	+.032	+.012	+.048	+.012	-.196	-.152	+.168	+.120
25 GSC(1)	157	22	26	200	1250	500	0	+.014	+.008	-.024	-.008	-.115	-.050	+.110	+.050
25 GSC(2)		45	46	2500	750	1600	0			+.012	0	-.152	-.072	+.136	+.040
25 GSC(3)		56	56	1500	750	1750	0	+.024	+.010	+.020	+.004	-.132	-.048	+.164	+.004
25 GSC(4)		63	68	1600	500	2250	500			+.024	+.004	-.128	-.040	+.188	+.088
25 GSC(5)		60	68	1500	500	2250	750	+.022	+.008	+.026	+.004	-.116	-.040	+.204	+.072

SERIES G - (BALLASTED) STEADY CURVING, REVERSE

	Curve Number	SPEED Min.	SPEED Max.	L_L Peak	L_L S.S.	L_R Peak	L_R S.S.	ΔY_{LF} Peak	ΔY_{LF} S.S.	ΔY_{RR} Peak	ΔY_{RR} S.S.	ΔX_{LF} Peak	ΔX_{LF} S.S.	ΔX_{RF} Peak	ΔX_{RF} S.S.
25 GSC(1R)	3	19	20	1250	250	0	0	-.016	-.008	-.032	-.016	-.130	-.060	+.140	.070
25 GSC(2R)		28	30	1000	250	750	0	-.016	-.008	-.032	-.020	-.124	.056	+.148	+.056
25 GSC(3R)		38	40	1000	0	1500	500			-.038	-.016	-.128	-.056	+.140	+.056
25 GSC(4R)		44	45	750	0	2000	750	-.020	-.008	-.044	-.016	-.124	-.056	+.128	+.040
25 GSC(5R)		48	50	600	0	3250	1250			-.056	-.016	-.104	-.040	+.132	+.040
25 GSC(1R)	311	10	12	1000	250	250	0	-.024	-.008	+.024	+.016	+.130	+.090	-.125	-.090
25 GSC(2R)		24	26	1250	500	0	0	+.016	+.004	+.030	+.020	+.104	+.056	-.128	-.080
25 GSC(3R)		34	36	1750	1000	0	0			+.040	+.024	+.128	+.080	-.128	-.088
25 GSC(4R)		39	42	2250	1250	0	0	+.024	+.012	+.040	+.024	+.112	+.072	-.128	-.088
25 GSC(5R)		40	44	2500	1500	250	0			+.062	+.032	+.125	+.064	-.136	-.088
25 GSC(1R)	37	10	12	1000	0	250	0	-.024	-.012	-.056	-.032	-.120	-.060	+.050	+.110
25 GSC(2R)		25	28	250	0	1250	500			-.048	-.028	-.136	-.088	+.148	+.080
25 GSC(3R)		34	38	0	0	2000	1000			-.040	-.024	-.144	-.080	+.144	+.080
25 GSC(4R)		35	46	250	0	4500	2000	-.050	-.024	-.042	-.024	-.164	-.080	+.104	+.064
25 GSC(5R)		36	49	500	0	4750	2000			-.044	-.012	-.144	-.064	+.168	+.080
25 GSC(1R)	43	20	20	2000	1000	0	0	+.020	+.008	-.036	-.016	-.080	-.505	+.090	+.060
25 GSC(2R)		40	40	1500	500	500	0			-.030	-.012	-.088	-.040	+.104	+.048
25 GSC(3R)		50	51	750	250	1250	250			-.026	-.010	-.104	-.048	+.112	+.048
25 GSC(4R)		60	61	500	0	2750	500	-.036	-.008	-.026	-.012	-.096	-.040	+.108	+.048
25 GSC(5R)		64	67	1000	250	3750	1000			-.024	-.008	-.104	-.064	+.092	+.048
25 GSC(1R)	49	15	17	1250	250	0	0	-.012	-.006	-.040	-.032	-.110	-.070	+.110	+.080
25 GSC(2R)		24	27	1000	0	750	0	-.040	-.012	-.050	-.032	-.124	-.072	+.136	+.080
25 GSC(3R)		44	44	500	0	1500	500			-.052	-.032	-.152	-.096	+.128	+.056
25 GSC(4R)		38	40	250	0	1750	750	-.052	-.012	-.048	-.028	-.108	-.056	+.136	+.072
25 GSC(5R)		46	47	250	0	3250	1500			-.056	-.028	-.120	-.064	+.104	+.056
25 GSC(1R)	157	24	27	2500	1500	0	0	+.020	+.008	+.024	+.004	-.050	-.030	+.070	+.035
25 GSC(2R)		44	47	2000	1250	600	0	-.022	-.004	-.032	-.012	-.080	-.040	+.064	+.032
25 GSC(3R)		52	58	2100	750	1000	0			-.032	-.012	-.092	-.048	+.046	+.016
25 GSC(4R)		64	68	1750	500	1750	500			-.038	-.010	-.092	-.056	+.052	+.008
25 GSC(5R)		69	72	1250	500	2000	500			-.034	-.012	-.076	-.048	+.056	+.016

SERIES G - ACCELERATION IN CURVES

Run	Curve	SPEED		L_L		L_R		ΔY_{LF}		ΔY_{RR}		ΔX_{LF}		ΔX_{RF}	
Number	Number	Max.	Min.	Peak	S.S.	Peak	S.S.	Peak	S.S.	Peak	S.S.	Peak	S.S.	Peak	S.S.
25-G-TR3P3	3	42	0	2600	750	4000	250	+.022	+.012	+.024	+.006	-.160	-.070	+.200	+.120
25-G-TR3P4	3	46	0	2100	1000	4500	500	+.026	+.008	+.028	+.008	-.165	-.060	+.230	+.150
25-G-TR37P3	37	34	0	3500	1750	4500	1500	+.022	+.008	+.020	+.008	-.170	-.100	+.210	+.170
25-G-TR37P4	37	46	0	4000	1750	5250	2000	+.026	+.008	+.038	+.012	-.190	-.900	+.230	+.200

SERIES G - STABILITY RUNS

Run Number	Speed (mph)		Peak Measurements - Absolute and Level Exceeded for 100 ms													
			L_L (kips)		L_R (kips)		$a_y A\text{-}1$ (g's)		$a_y A\text{-}2$ (g's)		$a_y A\text{-}3$ (g's)		$\Delta_y LF$ (in)		$\Delta_y RR$ (in)	
	min	max	abs	100ms	abs	100ms	abs	100ms	abs	100ms	abs	100ms	abs	100ms	abs	100ms
25GST(35)	33	36	1000	600	2000	500	-.14	-.04	+.14	+.04	+.12	+.06			+.016	+.012
25GST(55)	55	56	1250	1000	2500	500	-.30	-.14	+.28	+.08	-.34	-.10			+.016	+.008
25GST(65)	64	67	1500	750	2750	250	-.40	-.16	+.32	-.16	-.42	+.14			+.010	+.008
25GST(75)	75	78	1750	750	3250	250	-.52	-.12	+.40	-.16	-.56	-.18			-.020	-.012
25GST(35R)	32	37	1100	750	600	500	+.12	+.04	+.20	+.04	+.12	+.04			+.018	+.014
25GST(65R)	66	66	1500	500	600	0	-.28	+.08	-.34	-.06	-.28	+.08			-.016	+.008
25GST(75R)	76	78	1500	1000	750	0	-.36	-.08	-.42	-.10	-.42	+.10			+.280	+.008

SERIES I - STEADY CURVING, FORWARD

	Curve Number	SPEED		L_L		L_R		ΔY_{LF}		ΔY_{RR}		ΔX_{LF}		ΔX_{RF}	
		Min.	Max.	Peak	S.S.	Peak	S.S.	Peak	S.S.	Peak	S.S.	Peak	S.S.	Peak	S.S.
31 ISC(1F)	3	14	22	3250	1750	4250	1250	+.026	+.014	+.022	+.012	-.032	-.026	+.048	+.040
31 ISC(2F)		22	23	3000	1500	4250	1000	+.028	+.016	+.022	+.012	-.036	-.028	+.050	+.040
31 ISC(3F)		40	46	2600	1500	6000	2000	+.032	+.020	+.024	+.012	-.040	-.032	+.048	+.040
31 ISC(4F)		36	48	2750	1250	6250	1750	+.018	+.012	+.028	+.012	-.048	-.036	+.040	+.032
31 IRE(F)		47	49	2500	1250	7100	2250	+.028	+.018	+.028	+.014	-.044	-.034	+.038	+.032
31 ISC(1F)	311	15	17	6400	3500	4000	3000	-.014	-.004	-.020	-.010	+.036	+.028	-.034	-.028
31 ISC(2F)		25	29	7500	3000	3750	2250	-.022	-.008	-.020	-.012	+.034	+.028	-.040	-.032
31 ISC(3F)		38	40	8000	4000	3750	2500	-.022	-.008	-.010	-.008	+.032	+.024	-.048	-.038
31 ISC(4F)		41	43	9000	4000	3000	2000	-.018	-.008	-.020	-.008	+.032	+.024	-.046	-.040
31 IRE(F)		44	45	9250	3750	2750	1750	-.020	-.010	-.018	-.010	+.024	+.020	+.052	+.044
31 ISC(1F)	37	14	19	5000	3250	7250	4000	+.020	+.012	+.020	+.008	-.036	-.028	+.052	+.048
31 ISC(2F)		26	27	4400	3000	7000	4000	+.024	+.016	+.018	+.008	-.044	-.036	+.052	+.046
31 ISC(3F)		36	40	4000	2750	8000	4500	+.032	+.024	+.024	+.012	-.048	-.038	+.052	+.046
31 ISC(4F)		38	42	4000	2750	8500	4000	+.024	+.016	+.020	+.008	-.044	-.036	+.050	+.044
31 IRE(F)		37	40	4000	2750	8500	4500	+.026	+.020	+.018	+.006	-.050	-.036	+.044	+.038
31 ISC(1F)	43	20	22	3500	2000	3500	750	+.020	+.012	+.018	+.010	-.028	-.020	+.044	+.038
31 ISC(2F)		40	41	2750	1750	4500	1000	+.020	+.012	+.020	+.012	-.038	-.028	+.040	+.032
31 ISC(3F)		53	54	3000	1500	5750	1250	+.018	+.008	+.022	+.012	-.036	-.028	+.040	+.034
31 ISC(4F)		64	66	2250	1250	6500	1000	+.022	+.012	+.020	+.012	-.040	-.028	+.042	-.032
31 IRE(F)		65	66	2250	1000	6750	1250	+.026	+.018	+.020	+.010	-.044	-.028	+.036	-.028
31 ISC(1F)	49	14	18	4000	2500	5000	2500	+.024	+.008	+.014	+.004	-.032	-.024	+.044	+.036
31 ISC(2F)		34	36	3750	2250	5250	2750	+.046	+.012	+.032	+.008	-.040	-.032	+.040	+.032
31 ISC(3F)		38	40	3400	2000	6600	3500	+.040	+.016	+.036	+.012	-.044	-.030	+.044	+.034
31 ISC(4F)		43	46	3000	2000	7000	3750	+.040	+.012	+.034	+.008	-.048	-.032	+.048	+.036
31 IRE(F)		45	45	3000	2000	7000	3500	+.048	+.012	+.032	+.004	-.050	-.036	+.044	+.032
31 ISC(1F)	157	26	27	3500	2000	2250	500	+.020	+.008	+.018	+.008	-.032	-.020	+.048	+.036
31 ISC(2F)		40	57	3000	1500	2500	500	+.024	+.008	+.022	+.008	-.040	-.024	+.046	+.028
31 ISC(3F)		43	62	3400	1750	2000	1000	+.020	+.012	+.024	+.008	-.035	-.020	+.048	+.036
31 ISC(4F)		40	62	3600	1750	3250	1000	+.018	+.006	+.018	+.006	-.032	-.016	+.050	+.038
31 IRE(F)		42	61	3600	1750	3400	750	+.026	+.010	+.016	+.004	-.034	-.018	+.042	+.032

LVDT STICKING

SERIES I - STEADY CURVING, REVERSE

	Curve Number	SPEED Min.	SPEED Max.	L_L Peak	L_L S.S.	L_R Peak	L_R S.S.	ΔY_{LF} Peak	ΔY_{LF} S.S.	ΔY_{RR} Peak	ΔY_{RR} S.S.	ΔX_{LF} Peak	ΔX_{LF} S.S.	ΔX_{RF} Peak	ΔX_{RF} S.S.
31 ISC(1R)	3	19	21	1000	0	750	0	-.022	-.016	-.018	-.008	-.016	-.010	+.014	+.010
31 ISC(2R)		30	32	750	0	1250	250	-.016	-.014	-.018	-.008	-.016	-.010	+.018	+.008
31 ISC(3R)		42	44	500	0	2100	1000	-.010	-.004	-.018	-.008	-.016	-.008	+.014	+.008
31 ISC(4R)		47	49	400	0	2400	1250	+.012	+.004	-.022	-.010	-.018	-.010	+.012	+.006
31 IRE(5R)		51	51	250	0	2750	1500	-.008	.000	-.024	-.012	-.016	-.010	+.012	+.004
31 ISC(1R)	311	15	16	1000	250	750	0	+.012	+.004	+.016	+.006	+.024	+.022	-.032	-.030
31 ISC(2R)		26	27	1500	500	250	0	+.016	+.006	+.018	+.008	+.024	+.022	-.032	-.032
31 ISC(3R)		38	39	2250	1250	600	0	+.020	+.008	+.026	+.010	+.028	+.024	-.030	-.024
31 ISC(4R)		44	45	2500	1500	0	0	+.020	+.008	+.024	+.012	+.024	+.020	-.032	-.030
31 IRE(5R)		42	45	2600	1500	0	0	+.010	+.004	+.022	+.008	+.028	+.024	-.032	-.028
31 ISC(1R)	37	14	18	1600	250	750	100	-.016	-.012	-.014	-.010	-.020	-.016	+.028	+.024
31 ISC(2R)		26	27	1000	0	1100	250	-.014	-.008	-.016	-.008	-.022	-.016	+.024	+.022
31 ISC(3R)		38	40	600	0	2250	1250	-.012	.000	-.020	-.010	-.030	-.020	+.020	+.016
21 ISC(4R)		40	42	600	0	2100	1500	-.018	-.004	-.030	-.008	-.024	-.018	+.028	+.020
31 IRE(5R)		32	41	900	0	2250	1000	+.012	+.004	-.020	-.008	-.026	-.018	+.022	+.014
31 ISC(1R)	43	22	22	1250	250	100	0	-.024	-.016	-.014	-.008	-.010	-.006	+.014	+.010
31 ISC(2R)		42	42	500	0	750	250	-.020	-.012	-.020	-.012	-.008	-.004	+.012	+.010
31 ISC(3R)		53	53	400	0	1600	750	-.008	-.002	-.016	-.010	-.012	-.004	+.010	+.006
31 ISC(4R)		52	53	500	0	1500	750	-.008	.000	-.018	-.012	-.008	-.004	+.018	+.012
31 IRE(5R)		53	58	250	0	1500	750	-.008	-.004	-.020	-.012	-.006	.000	+.016	+.008
31 ISC(1R)	49	14	16	2100	1000	0	0	-.032	-.020	-.032	-.012	-.024	-.016	+.038	+.032
31 ISC(2R)		24	26	1500	500	500	0	-.024	-.004	-.024	.000	-.020	-.012	+.024	+.022
31 ISC(3R)		38	38	1000	0	1400	500	-.014	-.004	-.018	-.004	-.020	-.016	+.022	+.018
31 ISC(4R)		42	43	750	0	2000	750	-.026	-.004	-.034	-.008	-.022	-.014	+.028	+.022
31 IRE(5R)		44	46	600	0	2250	1250	-.026	-.004	-.032	-.006	-.020	-.014	+.024	+.016
31 ISC(1R)	157	27	29	2250	1000	250	0	-.022	-.012	-.016	-.008	-.018	-.008	+.030	+.020
31 ISC(2R)		46	48	2000	500	500	0	-.020	-.008	-.002	.000	-.018	-.008	+.022	+.012
31 ISC(3R)		52	61	2100	500	1500	500	-.018	-.006	-.024	-.008	-.016	-.004	+.024	+.012
31 ISC(4R)		60	65	2100	500	1750	750	-.012	-.004	-.018	-.006	-.018	-.008	+.024	+.012
31 IRE(5R)		62	65	1750	500	1500	750	-.010	-.004	-.018	-.004	-.012	-.004	LVDT STICKING	

SERIES I - ACCELERATION IN CURVES

Run Number	Curve Number	SPEED		L_L		L_R		ΔY_{LF}		ΔY_{RR}		ΔX_{LF}		ΔX_{RF}	
		Max.	Min.	Peak	S.S.	Peak	S.S.	Peak	S.S.	Peak	S.S.	Peak	S.S.	Peak	S.S.
31-I-TR3P3	3	44	0	3750	2500	5600	2000	+.016	+.008	+.022	+.008	-.030	-.020	+.042	+.036
31-I-TR3P4	3	52	0	4250	2500	6000	2500	+.010	+.004	+.020	+.008	-.030	.016	+.044	+.036
31-I-TR37P3	37	28	0	5250	4500	8250	4500	+.026	+.008	+.014	+.004	-.030	-.020	+.038	+.034
31-I-TR37P4	37	42	0	5000	4500	8100	4500	+.008	+.004	+.016	+.004	-.044	-.020	+.042	+.036

SERIES I - STABILITY RUNS

Peak Measurements - Absolute and Level Exceeded for 100 ms

Run Number	Speed (mph) min	Speed (mph) max	L_L (kips) abs	L_L (kips) 100ms	L_R (kips) abs	L_R (kips) 100ms	a_yA-1 (g's) abs	a_yA-1 (g's) 100ms	a_yA-2 (g's) abs	a_yA-2 (g's) 100ms	a_yA-3 (g's) abs	a_yA-3 (g's) 100ms	Δ_y^{LF} (in) abs	Δ_y^{LF} (in) 100ms	Δ_y^{RR} (in) abs	Δ_y^{RR} (in) 100ms
31IST(35F)	36	38	1500	500	2250	500	+.18	+.04	+.10	+.04	+.14	+.04	+.024	+.016	+0.20	+.012
31IST(55)	57	58	1600	1000	3250	250	+.28	+.06	+.26	+.04	+.26	+.04	+.016	+.008	+0.16	+.008
31IST(65)	64	68	1750	1000	3100	250	.30	.06	.28	.06	.30	.08	.016	.008	.012	.008
31IST(75)	60	75	1900	750	3250	250	.32	.08	.32	.06	.32	.08	.020	.012	.012	.006
31IST(35R)	36	38	1750	1000	500	0	+.12	+.02	+.16	+.02	+.14	+.04	+.018	+.012	+.018	+.008
31IST(55R)	56	60	2000	1100	500	0	+.20	-.04	.22	+.02	.18	.06	+.022	+.008	+.020	+.012
31IST(65R)	58	70	2000	1000	750	0	.22	.04	.26	.06	.20	.04	.020	.008	.018	.008
31IST(75R)	63	74	1900	1000	750	0	.22	.04	.26	.04	.22	.04	.022	.008	.016	.006

SERIES J - STEADY CURVING, FORWARD

	Curve Number	SPEED		L_L		L_R		ΔY_{LF}		ΔY_{RR}		ΔX_{LF}		ΔX_{RF}	
		Min.	Max.	Peak	S.S.	Peak	S.S.	Peak	S.S.	Peak	S.S.	Peak	S.S.	Peak	S.S.
7 JSC(1)	3	20	20	3000	1250	3750	1750			-.028	-.010	-.180	-.080	+.190	+.090
7 JSC(2)		30	28	2600	1000	4500	2000			-.024	-.008	-.185	-.080	+.180	+.060
7 JSC(3)		41	38	2600	750	5250	2750			+.022	.000	-.200	-.080	+.175	+.070
7 JSC(4)		43	46	2250	1000	6250	3000			+.036	+.008	-.215	-.060	+.195	+.080
7 JRE(F)		44	45	2000	500	5500	2750			+.026	+.006	-.155	-.050	+.190	+.080
7 JSC(1)	311	12	15	5500	3500	3750	2500			-.024	-.008	+.170	+.080	-.125	-.050
7 JSC(2)		22	23	6000	4000	3250	2000			-.020	-.008	+.145	+.060	-.165	-.080
7 JSC(3)		32	33	6500	4500	3000	1750			-.036	-.012	+.155	+.080	-.155	-.070
7 JSC(4)		37	40	7400	4500	2600	1500			-.028	-.012	+.120	+.045	-.125	-.050
7 JRE(F)		36	41	8250	5000	2750	1750			-.042	-.018	+.165	+.070	-.165	-.070
7 JSC(1)	37	12	18	3000	1400	5250	2500			-.024	-.008	-.170	-.090	+.210	+.140
7 JSC(2)		23	26	3250	1500	6100	3250			+.016	.000	-.175	-.100	+.180	+.100
7 JSC(3)		31	34	2750	1000	6500	3500			+.026	+.004	-.170	-.080	+.195	+.120
7 JSC(4)		12	38	3250	1500	7500	3250			+.022	+.006	-.230	-.090	+.205	+.130
7 JRE(F)		35	38	2600	1000	8000	3750			+.022	+.006	-.190	-.090	+.190	+.120
7 JSC(1)	43	14	18	3750	2250	4000	2000			-.034	-.018	-.130	-.040	+.165	+.060
7 JSC(2)		37	38	3000	1700	5500	2250			+.014	+.002	-.135	-.050	+.145	+.025
7 JSC(3)		48	49	3000	1500	6000	2500			-.024	-.008	-.120	-.040	+.145	+.040
7 JSC(4)		53	54	2750	1250	6600	2500			-.020	-.006	-.150	-.050	+.210	+.050
7 JRE(F)		60	62	2250	1000	7750	3000			+.044	+.012	-.150	-.030	+.190	+.030
7 JSC(1)	49	12	16	3500	1250	5000	1750			-.028	-.010	-.160	-.110	+.190	+.120
7 JSC(2)		22	24	3750	1250	6000	2250			-.032	-.006	-.180	-.110	+.160	+.090
7 JSC(3)		44	44	3000	750	5750	2750			+.026	+.004	-.190	-.100	+.180	+.100
7 JSC(4)		36	39	2900	1000	6100	3250			+.022	+.004	-.190	-.120	+.210	+.130
7 JRE(F)		40	41	2750	750	7000	3500			+.032	+.008	-.200	-.100	+.175	+.100
7 JSC(1)	157	22	25	3500	2000	2750	1250			-.040	-.012	-.110	-.040	+.080	+.010
7 JSC(2)		44	46	2750	1750	4000	1500			-.024	-.008	-.105	-.040	+.075	.000
7 JSC(3)		54	56	2500	1250	4000	1500			-.022	-.008	-.095	-.020	+.080	+.010
7 JSC(4)		40	58	3000	1500	4500	2000			-.028	-.010	-.085	-.010	+.140	+.060
7 JRE(F)		39	52	2750	1500	4000	1750			-.026	-.010	-.095	-.010	+.110	+.030

SERIES J - STEADY CURVING, REVERSE

	Curve Number	SPEED		L_L		L_R		ΔY_{LF}		ΔY_{RR}		ΔX_{LF}		ΔX_{RF}	
		Min.	Max.	Peak	S.S.	Peak	S.S.	Peak	S.S.	Peak	S.S.	Peak	S.S.	Peak	S.S.
7 JSC(1R)	3	17	19	2100	1000	1500	250			+.042	+.010	-.150	-.080	+.175	+.100
7 JSC(2R)		27	28	2000	750	2000	5000			+.046	+.018	-.130	-.065	+.165	-.080
7 JSC(3R)		38	38	1500	500	2500	1000			+.052	+.024	-.145	-.070	+.150	+.080
7 JSC(4R)		44	44	1500	250	3600	1500			+.046	+.012	-.140	-.055	+.125	+.055
7 JRE(R)		48	49	1000	250	4400	1500			+.048	+.016	-.160	-.060	+.100	+.040
7 JSC(1R)	311	9	15	750	0	750	0			-.028	-.012	+.225	+.170	-.200	-.155
7 JSC(2R)		24	24	1100	0	750	0			-.044	-.020	+.220	+.180	-.195	-.160
7 JSC(3R)		34	36	2000	500	250	0			-.044	-.020	+.220	+.170	-.210	-.170
7 JSC(4R)		39	41	2400	1000	200	0			-.058	-.032	+.210	+.160	-.210	-.160
7 JRE(R)		28	30	1250	250	600	0			-.044	-.020	+.220	+.170	-.195	-.160
7 JSC(1R)	37	14	16	2000	500	1750	250			+.036	+.012	-.160	-.100	+.180	+.120
7 JSC(2R)		25	30	1500	250	2500	750			+.046	+.016	-.160	-.090	+.195	+.130
7 JSC(3R)		32	39	1000	0	4200	1500			+.060	+.028	-.160	-.080	+.185	+.110
7 JSC(4R)		30	37	1700	250	3900	1250			+.052	+.012	-.190	-.100	+.105	+.100
7 JRE(R)		36	37	1200	0	4000	1500			+.050	+.020	-.190	-.090	+.165	+.100
7 JSC(1R)	43	18	20	2750	1500	1000	0			+.024	+.006	-.085	-.055	+.120	+.050
7 JSC(2R)		39	39	2500	1000	2750	500			+.032	+.010	-.095	-.045	+.120	+.050
7 JSC(3R)		48	48	2250	1000	3000	1000			+.032	+.006	-.105	-.030	+.110	+.040
7 JSC(4R)		44	46	2400	1000	2500	1000			+.024	+.008	-.100	-.045	+.110	+.035
7 JRE(R)		49	49	2500	750	3000	1000			+.052	+.008	-.085	-.035	+.090	+.040
7 JSC(1R)	49	13	15	2000	750	1500	0			+.032	+.008	-.160	-.100	+.160	+.110
7 JSC(2R)		22	2	2000	500	2500	250			+.036	+.012	-.170	-.100	+.175	+.115
7 JSC(3R)		32	36	1100	0	3200	750			+.036	+.012	-.160	-.090	+.150	+.090
7 JSC(4R)		38	39	1000	0	3750	1250			+.042	+.012	-.190	-.100	+.155	+.090
7 JRE(R)		40	42	1000	0	4250	1250			+.052	+.032	-.195	-.090	+.140	+.070
7 JSC(1R)	157	24	28	2500	1250	1000	0			+.024	+.004	-.070	-.140	+.060	+.025
7 JSC(2R)		46	46	2500	1000	1750	250			+.046	+.012	-.060	-.030	+.045	+.015
7 JSC(3R)		48	56	2100	1000	2100	500			+.044	+.016	-.050	-.010	+.070	+.030
7 JSC(4R)		58	61	2000	1000	3250	1000			+.040	+.008	-.080	-.040	+.040	+.010
7 JRE(R)		46	48	1500	750	3100	1500			+.040	+.016	-.110	-.040	+.070	+.025

SERIES J - STEADY CURVING AT AN UNWORN BLUELINE CURVE

	Curve Number	SPEED		L_L		L_R		ΔY_{LF}		ΔY_{RR}		ΔX_{LF}		ΔX_{RF}	
		Min.	Max.	Peak	S.S.	Peak	S.S.	Peak	S.S.	Peak	S.S.	Peak	S.S.	Peak	S.S.
2 JCA(6A)1	6	35	37	2750	1250	7250	4000	-.016	-.004	-.022	-.006	-.153	-.080	+.145	+.090
2 JCA(6B)2		35	37	2750	1250	7500	4000	-.022	-.004	-.022	-.004	-.165	-.085	+.160	+.100
2 JCA(6C)3		35	38	2750	1250	7600	4000	-.022	-.006	*	*	-.150	-.080	+.165	+.100
2 JCA(6D)4		36	38	2750	1250	7000	4250	-.022	-.006			.160	-.090	+.165	+.090
5															

*Not valid. The LVDT was loose, lost completely during next run.

SERIES J - ACCELERATION IN CURVES

Run Number	Curve Number	SPEED		L_L		L_R		ΔY_{LF}		ΔY_{RR}		ΔX_{LF}		ΔX_{RF}	
		Max.	Min.	Peak	S.S.	Peak	S.S.	Peak	S.S.	Peak	S.S.	Peak	S.S.	Peak	S.S.
7-J-TR3P3	3	40	0	3500	1500	5000	2500			-.024	-.006	-.140	-.040	+.195	+.100
7-J-TR3P4	3	48	0	3750	1500	6000	2500			-.024	-.008	-.080	-.020	+.220	+.130
7-J-TR37P3	37	32	0	3250	1500	5750	3000			-.020	-.004	-.160	-.070	+.220	+.140
7-J-TR37P4	37	40	0	4000	1500	6500	3000			-.024	-.004	-.200	-.040	+.225	+.170

SERIES J - STABILITY RUNS

Run	Speed (mph)		Peak Measurements - Absolute and Level Exceeded for 100 ms													
			L_L (kips)		L_R (kips)		a_yA-1 (g's)		a_yA-2 (g's)		a_yA-3 (g's)		$\Delta_y LF$ (in)		$\Delta_y RR$ (in)	
Number	min	max	abs	100ms	abs	100ms	abs	100ms	abs	100ms	abs	100ms	abs	100ms	abs	100ms
7-JST(35F)	35	37	3000	1750	4500	2000	.20	.08	.16	.02	.22	.06	+.016	+.012	+.016	+.012
7-JST(55F)	48	58	2900	1250	4000	1750	.36	.04	.24	.02	.32	.04	+.014	+.008	+.020	+.012
7-JST(65F)	52	59	3250	1250	5500	2000	.40	.12	.30	.04	.54	.06	+.016	+.008	+.024	+.010
7-JST(75F)	64	75	4200	1250	5400	2000	.50	.04	.38	.04	.52	.08			+.022	+.010
7-JST(35R)	34	38	1600	600	750	0	.16	0	.32	.04	.18	0	-.020	-.016	-.018	-.012
7-JST(55R)	56	58	1500	500	1000	0	.42	.04	.56	.06	.34	.04	-.036	-.030	-.024	-.020
7-JST(65R)	60	68	1250	500	1250	0	.52	.04	.62	.06	.34	.06	-.014	-.008	-.018	-.014
7-JST(75R)	70	75	1500	500	750	0	.54	.04	.62	.08	.36	.04			-.022	-.012

APPENDIX C REPORT OF NEW TECHNOLOGY

This report describes analyses and tests of wheel taper and primary suspension stiffness on wheel-rail interaction forces. The work described has not resulted in the development of any new or unique devices.